AD-A190 110 LINEAR STATE SPACE MODELING OF A TURBOFAN ENGINE(U) AIR FORCE INST OF TECH WRIGHT-PATTERSON AFB OH SCHOOL OF ENGINEERING G L THELEN DEC 87 AFIT/GA/AA/87D-10 1/1

UNCLASSIFIED F/G 21/5 NL

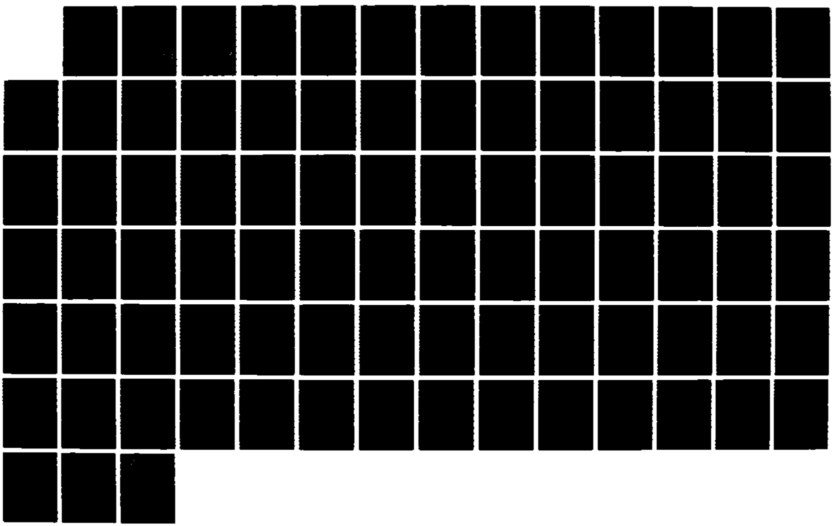

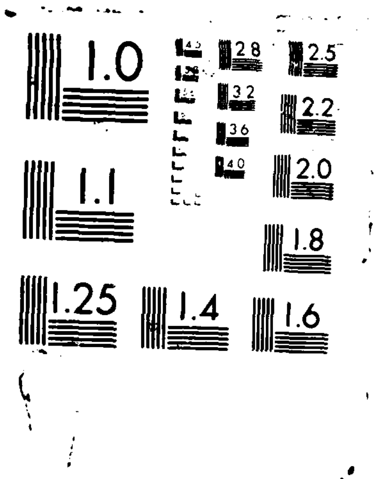
1.0
2.8
2.5
3.2
2.2
3.6
4.0
2.0
1.1
1.8
1.25
1.4
1.6

(1)

LINEAR STATE SPACE MODELING
OF A TURBOFAN ENGINE

THESIS

Gregory L. Thelen
Captain, USAF

AFIT/GA/AA/87D-10

DEPARTMENT OF THE AIR FORCE
AIR UNIVERSITY
AIR FORCE INSTITUTE OF TECHNOLOGY

Wright-Patterson Air Force Base, Ohio

AFIT/GA/AA/87D-10

LINEAR STATE SPACE MODELING
OF A TURBOFAN ENGINE

THESIS

Gregory L. Thelen
Captain, USAF

AFIT/GA/AA/87D-10

AFIT/GA/AA/87D-10

LINEAR STATE SPACE MODELING OF A TURBOFAN ENGINE

THESIS

Presented to the Faculty of the School of Engineering
of the Air Force Institute of Technology
Air University
In Partial Fulfillment of the
Requirements for the Degree of
Master of Science in Astronautical Engineering

Gregory L. Thelen, B.S.
Captain, USAF

December 1987

Approved for public release; distribution unlimited

Preface

The purpose of this study was to develop a technique to linearize a non-linear turbofan engine into linear state space format. The need for this study arose from the desire to better understand state-of-the-art engine control by development of accurate linear state space models.

To develop the linear state space models, I used a non-linear turbofan engine simulation, commonly referred to as a cycle deck. The turbofan engine simulation used in this study was for the F101 engine in use on the B-1B aircraft. Although the F101 engine is used in this particular study, the methodology for the development of linear state space models is valid for other turbofan engines.

I would very much like to thank Dr. Robert Calico for his patience and guidance, not just on the writing of this thesis, but for all of the classes I have taken from him and all the knowledge and insights he has given me. I have drawn on that knowledge many times and will continue in the future. Thank you. I would also like to thank my branch, ASD/ENFPA, in allowing me the use of computer resources and time to complete this study. In particular, Russel Denney. His keen understanding of engine simulation models was a constant source for me in understanding the intricate coding that makes up a non-linear engine simulation model.

Gregory L. Thelen

Table of Contents

List of Figures

List of Tables

TABLE OF SYMBOLS
AND
ENGINE STATION DESIGNATIONS

T_i	Temperature at Station (i)
P_i	Pressure at Station (i)
m_i	Mass Air Flow Rate at Station (i)
Station (i)	
1	Inlet Entrance
2	Low Pressure Fan Inlet
13	Forward Duct Bypass
16	Aft Duct Bypass
25	High Pressure Compressor Inlet
3	Combuster Inlet
4	High Pressure Turbine Inlet
42	Low Pressure Turbine Inlet
5	Low Pressure Turbine Exit
8	Nozzle Throat

Abstract

Present generation turbofan engines use hydro/mechanical control governors to regulate fuel flow and control engine performance. State-of-the -art and future engines will have the ability to use digital control logic to control engine performance. Due to these advances in engine control capability, there is a need to linearly model the turbofan engines and develop control systems to understand and optimize engine performance. This paper will describe the means of developing linear state space models which model transient turbofan engine performance.

The F101 turbofan engine, used on the B-1B bomber, will be used as the example with the linear state space models being derived from the non-linear F101 engine computer simulation model. The internal convergence logic of the F101 engine simulation will be used to derive the individual elements making up the linear state space models. The linear state space models will consist of both high speed and low speed rotor dynamics and turbine inlet temperature heat soak dynamics. State space inputs considered will be fuel flow and engine exit nozzle area. Also dicussed in this paper will be linear analyitic equations in state space format and their comparative accuracies to the models derived using the F101 non-linear computer simulation model.

Based on the linear state space models developed in this paper, control systems will be designed and implemented into the F101 engine computer model. Transient performance will be compared between current engine control design and the control design based on the linear state

space models. Final results will confirm the validity of the state space models derived by showing improvement over current engine transient performance.

LINEAR STATE SPACE MODELING OF A TURBOFAN ENGINE

I. Introduction

The dynamic response of turbofan engine systems may be accurately analyzed with modern state space techniques. Recent advances in engine technology, such as the extensive use of variable geometry and digital electronic controls, are ideally suited to state space analysis. However, developement of a state space model can be challanging. The difficulty in developing linear models lies in the use of non-linear thermodynamic computer engine models, commonly referred to as cycle decks. Cycle decks are usually purchased by the Air Force from the engine manufacturer. Engine modeling techniques can vary greatly from manufacturer to manufacturer which makes it very difficult to develop a generic method of using the non-linear cycle decks from the different engine manufacturers in deriving linear state space models. There are, however, some common denominators in engine thermodynamic modeling among manufacturers that serve as a basis in the development of linear state space models from non-linear cycle decks.

This paper will first examine how non-linear cycle decks thermodynamically model engine dynamics using a simple turbojet as an example. The results will be analogous to the more complex turbofan. A non-linear turbofan cycle deck will then be used to derive linear models. Also discussed in this paper will be the use of linear analytic equations to model the thermodynamic processes within the

engine. Finally, using the developed linear models, a rate feedback design which takes advantage of present digital technology will be shown to improve engine response characteristics over present day hydro/mechanical engine control designs used in the F101/B-1B turbofan engine.

II Non-linear Cycle Deck

A non-linear cycle deck thermodynamically balances pressures, temperatures, and flows across various engine components, the most common being the engine inlet, low pressure fan (LPF), high pressure compressor (HPC), high pressure turbine (HPT), the low pressure turbine (LPT) and the exhaust nozzle. The cycle deck satisfies both energy and flow continuity requirements based on inlet, fan, compressor, combustor, turbine and nozzle component characteristics predefined from experimental testing. The component characteristics are mapped (defined) as functions of temperature, pressure, and mass flow rates and integrated into the thermodynamic processes and calculations internal to the cycle deck computor simulation. Therefore, the cycle deck engine simulation models individual components with unique temperature, pressure and flow characteristics and through energy and flow continuity relationships establish their interdependence. To simplify the discussion of internal thermodynamic balancing of a non-linear engine cycle deck, a simple turbojet will be considered .

Turbojet Engine

Figure 1 is a representation of a turbojet engine consisting of a compressor, combustor, turbine and nozzle. All pressures and temperatures are absolute unless otherwise indicated, and the inlet is considered isentropically ideal. Also shown are component characteristic mappings of the compressor, turbine, and nozzle. Combustor efficiency (P_4/P_3) is a function of temperature, pressure, and geometry of the combustor and is considered defined from a table look-up

SIMPLE TURBOJET

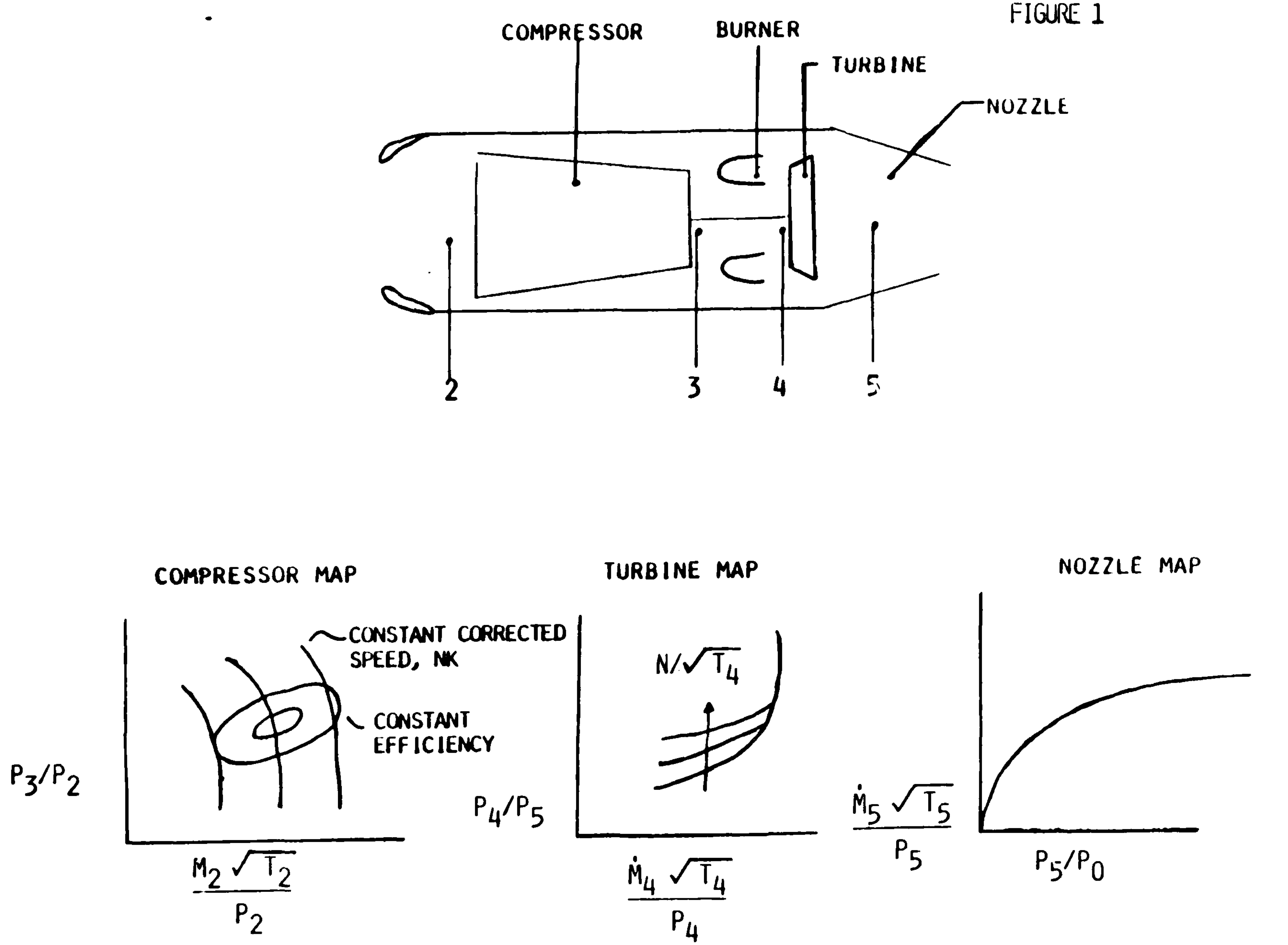

FIGURE 1

once the thermodynamic states are known at Station 3.

The power lever angle (PLA), or engine throttle position, defines the demanded, corrected, engine shaft speed, N_k. In the F1Ø1/B-1B and the F11Ø/F-15 turbofan engines, the schedule is imposed on a mechanical cam linked to the PLA position. For a given PLA setting, the engine will operate somewhere along a constant corrected speed line, N_k, at some operating point defined by the compressor map (see Figure 1). Any point along a given N_k will define a mass flow rate, pressure ratio, and efficiency across the compressor. An initial guess is made by the engine cycle deck program as to where along the N_k line the engine will operate defining the corresponding pressure ratio, P_{25}/P_3, corrected mass flow rate, m_{25k}, defined as $m_{25}\sqrt{T_{25}}/P_{25}$, and efficiency, η_c, across the compressor. It is assumed that inlet conditions, T_{25} and P_{25} are always known from instrumentation in the inlet. An expression for the compressor work in terms of temperature differences across the compressor and based on the guessed operating point on the compressor map is given in Equation (1) as,

$$T_{25} - T_3 = \frac{T_{25}}{\eta_c}\left[\left(\frac{P_3}{P_{25}}\right)^{\frac{\gamma - 1}{\gamma}} - 1\right] \qquad (1)$$

where γ is a function of temperature and fuel/air ratio, f. Compressor work and T_3 are now defined.

Thermodynamic properties equating T_3 and T_4 across the combustor can be written as,

$$(1 + f)C_{p4}T_4 = C_{p3}T_3 + f\eta_b Q \qquad (2)$$

where, C_p = Specific heat

η_b = Combustor efficiency

Q = Heating value of fuel.

The cycle deck guesses a value for f and given T_3 from Equation (1), Equation (2) may be solved for T_4. Recalling the values for N_k, defined by PLA position, and m_4, defined from f and m_2, P_4, defined from P_3 and η_b, and T_4, the turbine pressure ratio, P_4/P_5, can be determined from the turbine map characteristics (Figure 1). Turbine work can now be calculated using the equation below.

$$T_4 - T_5 = \eta_t T_4 \left[1 - \left(\frac{1}{P_4/P_5} \right)^{\frac{\gamma-1}{\gamma}} \right] \tag{3}$$

For steady state operation, the work being done across the compressor must be equal to the work across the turbine or acceleration in rotor speed will occur. If, based on the guessed fuel/air ratio, f, the compressor and turbine work are not equal, fuel/air ratio will be used to iterate between Equations (2) and (3) until the the compressor and turbine work are balanced.

The nozzle pressure ratio, P_5/P_o, and the nozzle corrected mass flow rate, $m_5\sqrt{T_5}/P_5$, can be calculated from the following equations:

$$P_5/P_o = (P_2/P_o)(P_3/P_2)(P_4/P_3)(P_5/P_4) \tag{4a}$$

where P_o is the ambient pressure , and

$$\frac{m_5\sqrt{T_5}}{P_5} = \frac{m_4\sqrt{T_4}}{P_4} \left(\frac{P_4}{P_5}\right)\left(\frac{T_5}{T_4}\right)^{1/2} . \tag{4b}$$

All the ratios on the right hand side of the above equations are known. However, P_5/P_o and the corrected mass air flow must also lie somewhere on the nozzle map (Figure 1). Continuity must be satisfied between calculated corrected mass flow rate and nozzle corrected mass flow rate characteristics. Recall that calculated values for P_5/P_o and corrected mass flow rate are based on the initially guessed compressor operating point. If the calculated nozzle corrected mass flow rate and the corrected mass flow rate based on the nozzle map characteristics do not match for a given P_5/P_o, a new compressor operatng point along the N_k speed line must be chosen until continuity is satisfied. Once satified, the entire thermodynamic cycle is satisfied for both energy and continuity.

Various techniques for iteration on fuel/air ratio and compressor operating line exist and vary from simplified techniques which can be accomplished on a hand-held calculator to more accurate methods which require the Newton-Raphson technique such as is currently used in General Electric engine cycle simulations[1], but the basic premise of energy and continuity satisfaction must always be met.

Turbofan Engine

Consider a turbofan as a high rotor speed turbojet surrounded by another low rotor speed turbojet. Stage by stage the thermodynamic energy equations are satisfied in the same manner as the simple turbojet example. Figure 2 shows a typical turbofan engine. The additional components distinguishing it from a turbojet are the low pressure fan, (LPF), low pressure turbine, (LPT), and the bypass duct. Like the turbojet, inlet conditions are known. Work across the LPF and LPT must

FIGURE 2 TURBOFAN ENGINE

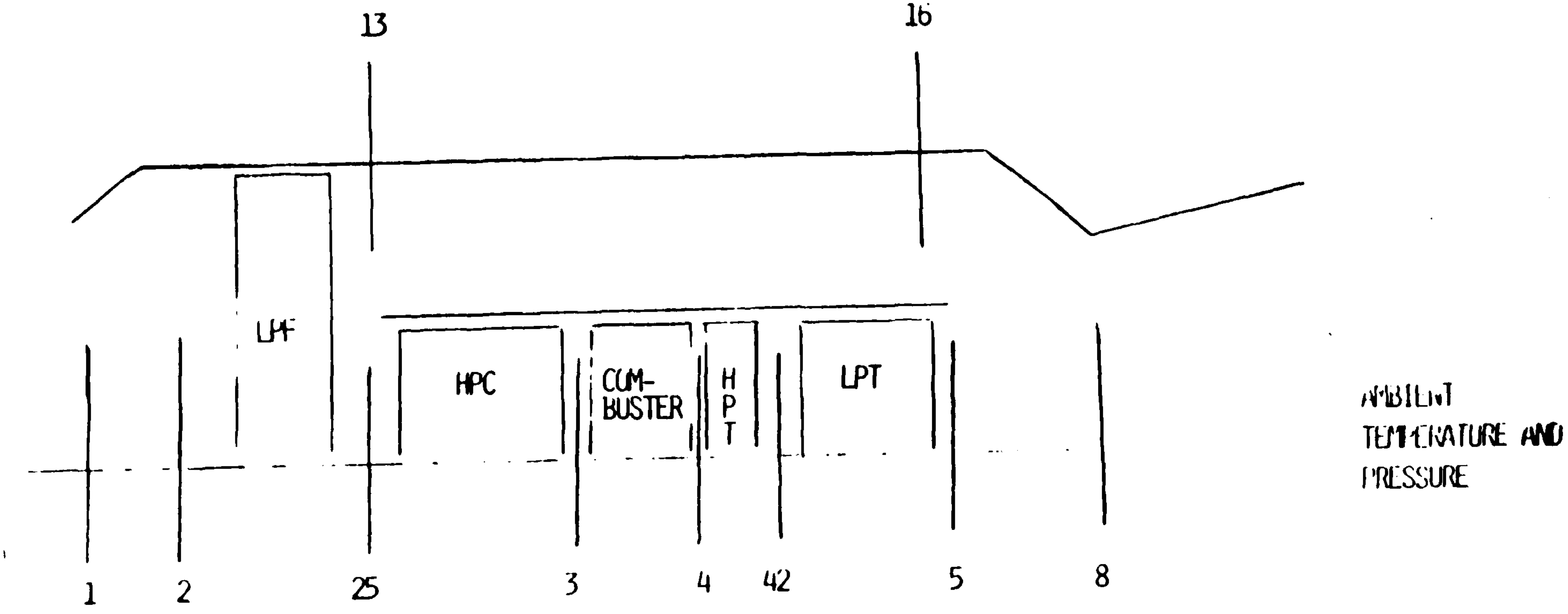

ENGINE STATION DESIGNATION

STATION	
1	ENTRANCE TO INLET
2	LPF INLET
13	FORWARD DUCT BYPASS
16	AFT DUCT BYPASS
25	HPC INLET
3	COMBUSTER INLET
4	HPT INLET
42	LPT INLET
5	LPT EXIT
8	NOZZLE AREA

TURBOFAN - A HIGH SPEED SPOOL SURROUNDED BY A LOW SPEED SPOOL

be equal just as work across the high pressure compressor, (HPC), and the high pressure turbine, (HPT). Also like the turbojet, an operating point for the LPF is guessed by assuming a bypass ratio (ratio of air through the duct divided by the air through the compressor) and low rotor speed. This serves to define a pressure ratio and corrected mass air flow across the LPF and in turn, inlet conditions into the HPC. Continuity is satisfied by requiring static pressures of the duct and high speed rotor mass flow rates at the mixing point of the duct and core be equal. The mass air flows mix shortly after station 5. Static pressures will be equal provided no shocks exist at the mixing point which is normally the case. The F101/B-1B assures this to be the case by scheduling duct Mach number as a function of engine inlet temperature. Duct mass flow velocity is controlled by varying nozzle exit area. Nozzle flow continuity of the combined duct and core mass air flow must also be satisfied based on nozzle map characteristics.

The energy and continuity conditions for a turbofan are satisfied in an analagous manner to those of a turbojet. The only real conceptual difference is in the number of energy and continuity conditions to be satisfied. The important point to realize is that in equilibrium, flow continuity is satisfied along with the work energy conditions. Any torque applied off equilibrium (off-torque) on either rotor would force a rematching of energy (spool work) and continuity within the engine to maintain equilibrium. The engine rematch would cause acceleration/deceleration to occur until equilibrium was once again obtained.

III Off-Torque in Turbofan Linearization

Off-Torque

Off-torque is defined as any torque applied to the high or low spool rotor that is different than the torque required to maintain equilibrium. Each engine equilibrium condition has associated equilibrium engine parameters. The parameters of most interest are N_{1e}, N_{2e}, T_{4e}, W_{fe}, and A_{8e}. For the turbofan engine, N_1 is defined as the low rotor speed; N_2 is the high rotor speed; T_4 is the HPT inlet temperature; W_f is the fuel flow and A_8 is the nozzle exit area. The importance of these particular parameters will be discussed shortly. Each of these parameters has an equilibrium value associated with it indicated by the subscript 'e'. However, if for example, N_1 was forced to operate at $(N_{1e}+dN_1)$ and the other four parameters remained unchanged, continuity and energy conditions would no longer be satisfied. The engine would have a desire to change both its rotor speeds and HPT inlet temperature to operate at the new equilibrium rotor speed $(N_{1e}+dN_1)$. The desire of the engine to rematch to a new equilibrium point can be used in a computer simulation model cycle deck to develop linear equations of motion.

Off-Torque Method

Using a cycle deck to force a turbofan to operate at an off-equilibrium point requires three new iteration parameters to force a new operating point defined by $(N_{1e}+dN_1)$, N_{2e}, and T_{4e}. W_f and A_8 are not allowed to change. The three iteration parameters used are low

speed spool off-torque, $\dot{N}_1$, high speed spool off-torque, $\dot{N}_2$, and a 'temperature off-torque', $\dot{T}_4$, made up by adding dT_4 to T_4 to obtain (T_4+dT_4) and multiplied by the turbine rotor heat soak constant, τ to give $\dot{T}_4$. The heat soak constant is a function of temperature and flow and is calculated within the cycle deck. It has units of 1/sec and, when multiplied by dT_4, gives $\dot{T}_4$. The three iteration parameters, $\dot{N}_1$, $\dot{N}$, and $\dot{T}$ are used to define the elements of the state space equation.

State Space Equation

The elements of the A and B matrices in the state space equation,

$$[\dot{X}] = [A][X] + [B][U],$$

are of the form,

$$A = \left| \frac{\partial \dot{X}_i}{\partial X_j} \right|_{i,j=1,3} \quad \text{and} \quad B = \left| \frac{\partial \dot{X}_i}{\partial U_k} \right|_{i=1,3;\ k=1,2}$$

where, for the above turbofan example,

$$X_1 = N_1 \qquad U_1 = W_f$$

$$X_2 = N_2 \qquad U_2 = A_8$$

$$X_3 = T_4.$$

The off-torques required for operation at an off-equilibrium point are $\dot{N}_1$, $\dot{N}_2$, and $\dot{T}_4$. Therefore, the first column of matrix A is defined as the off-torques required to rebalance an off-equilibrium point of $(N_{1e}+ dN_1)$, N_{2e}, and T_{4e} for a given W_f and A_8, divided by dN_1. The second column of A is similarly defined by the off-equilibrium point of N_{1e}, $(N_{2e}+ dN_2)$, and T_{4e} for a given W_{fe} and A_8. The last column of A is completed using $(T_{4e}+dT_4)$, and the columns of the B matrix are

completed using (W_{fe}+ dW_f) and (A_8+ dA_8) and the off-torques required to run to their respective off-equilibrium points. Thus, the state space equation linearly modeling a turbofan engine about small changes from the equilibrium is complete.

State Space Parameters

It is not initially evident why the state space parameters N_1 N_2, and T_4 are used in describing the dynamics of a turbofan engine. In short, the methods of choosing the proper engine parameters depends on the speed of response of the internal engine dynamics, the degree of accuracy required in the state space model and which parameters are of interest. As an example, pressure within the nozzle, P_8 becomes important in describing engine dynamics when a long nozzle is involved. The longer nozzle allows the relatively high speed pressure dynamics to significantly affect transient conditions. For the F101/B-1B engine used as the example in this paper, P_8 dynamics are very quick relative to the length of the nozzle and do not appreciably add to the dynamic model. However, on some engines, like the F100/F15,F16, P_8 dynamics do play a role in modeling the dynamics.

Turbine inlet temperature is an important parameter in the F101/B-1B engine because of the large HPT disk heat soak characteristics. The dynamics of the heat soaked into the disk significantly affect temperatures and pressures down stream of the HPT. Therefore, the heat soak time constant plays a substantial role in engine transient dynamics. Naturally, the parameters N_1 and N_2 are always of interest because the inertias involved with the low and high speed spools dramatically affect transient acceleration times.

The size of the deltas dN_1, dN_2, and dT_4 will vary in magnitude for accurate off-torque results. If the delta size is too small the algebraic limitations of the cycle would not converge on an accurate off-torque value. If the delta size is too large, the off-torque due to a positive delta would not equal in magnitude the off-torque due to a negative delta. Delta sizes will vary for different PLA settings and from engine to engine.

State Space Model Results

The non-linear transient engine cycle deck model for the F101/B-1B was used to generate the state space model. Internal cycle deck logic was developed to manipulate the Newton-Raphson convergence subroutines to use off-torques in rebalancing to new off-equilibrium points. State space models were developed at various PLA positions (equilibrium points) in small 5 degree increments for accurate model continuity between PLA points. Figures 3 through 10 show the root locus and gain/phase plots for the N_2/W_f transfer function derived from the various state space models. The N_2/W_f transfer function is of most interest in designing a control scheme since the F101/B-1B engine uses N_2 schedules to set fuel flow, W_f, for given throttle settings. Present engine transient control logic uses N_2 as a gain feedback.

Notice the characteristics of the root locus plots. In all cases there are two zeros and three poles, one pair as a complex conjugate. One zero is relatively large and the other situated near a pole. The complex pole conjugates are located nearest the imaginary axis. These characteristics of relative root and pole location are consistent at each throttle position.

FIGURE 3A OLTF N_2/W_F ROOT LOCUS FOR PLA=35 DEG

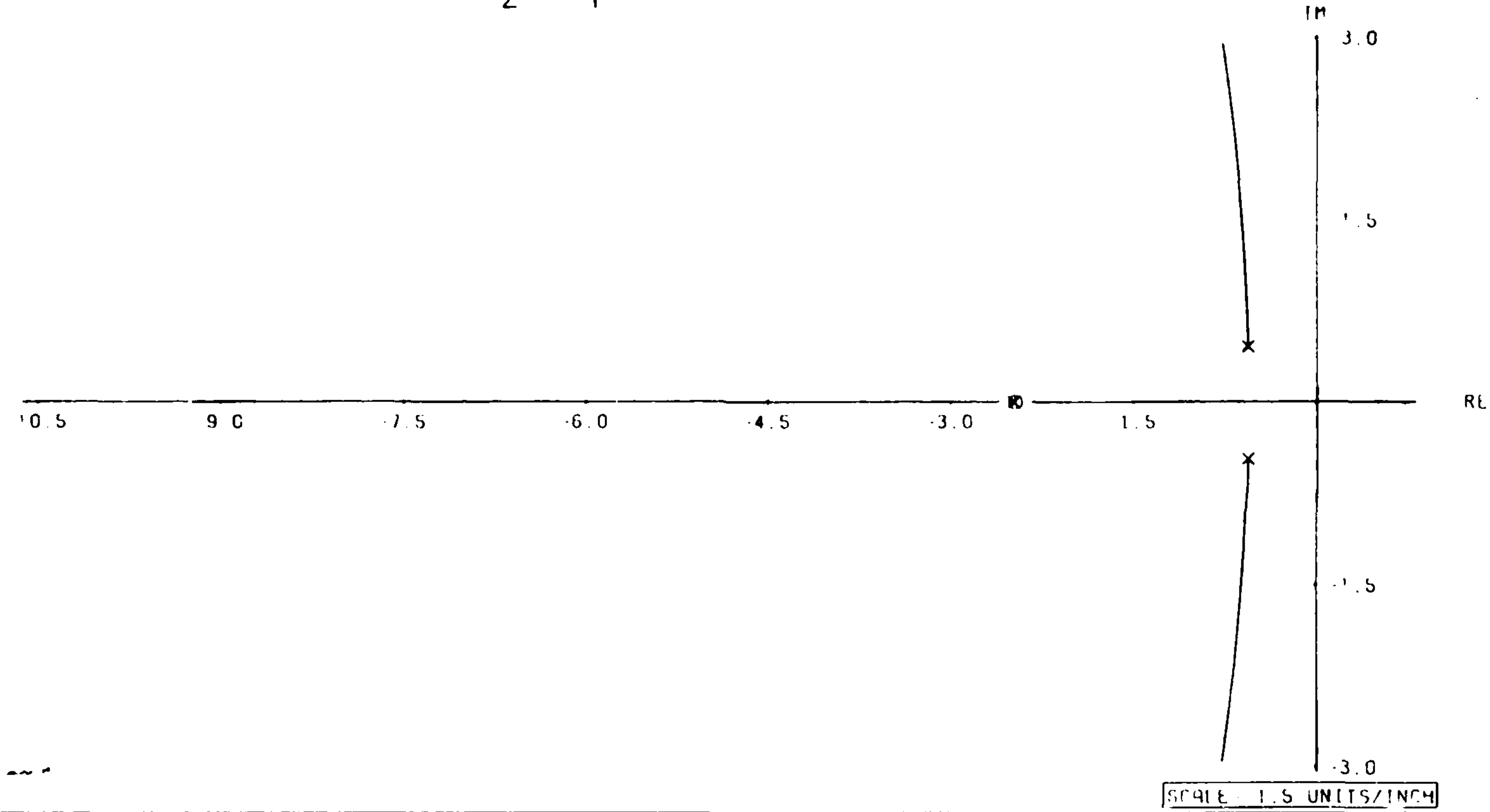

$$OLTF(S) = \frac{K(S+2.470)(S+21.572)}{(S+2.485)(S^2+1.119S+0.527)}$$

FIGURE 3B OLTF N_2/W_F BODE PLOT FOR PLA=35 DEG

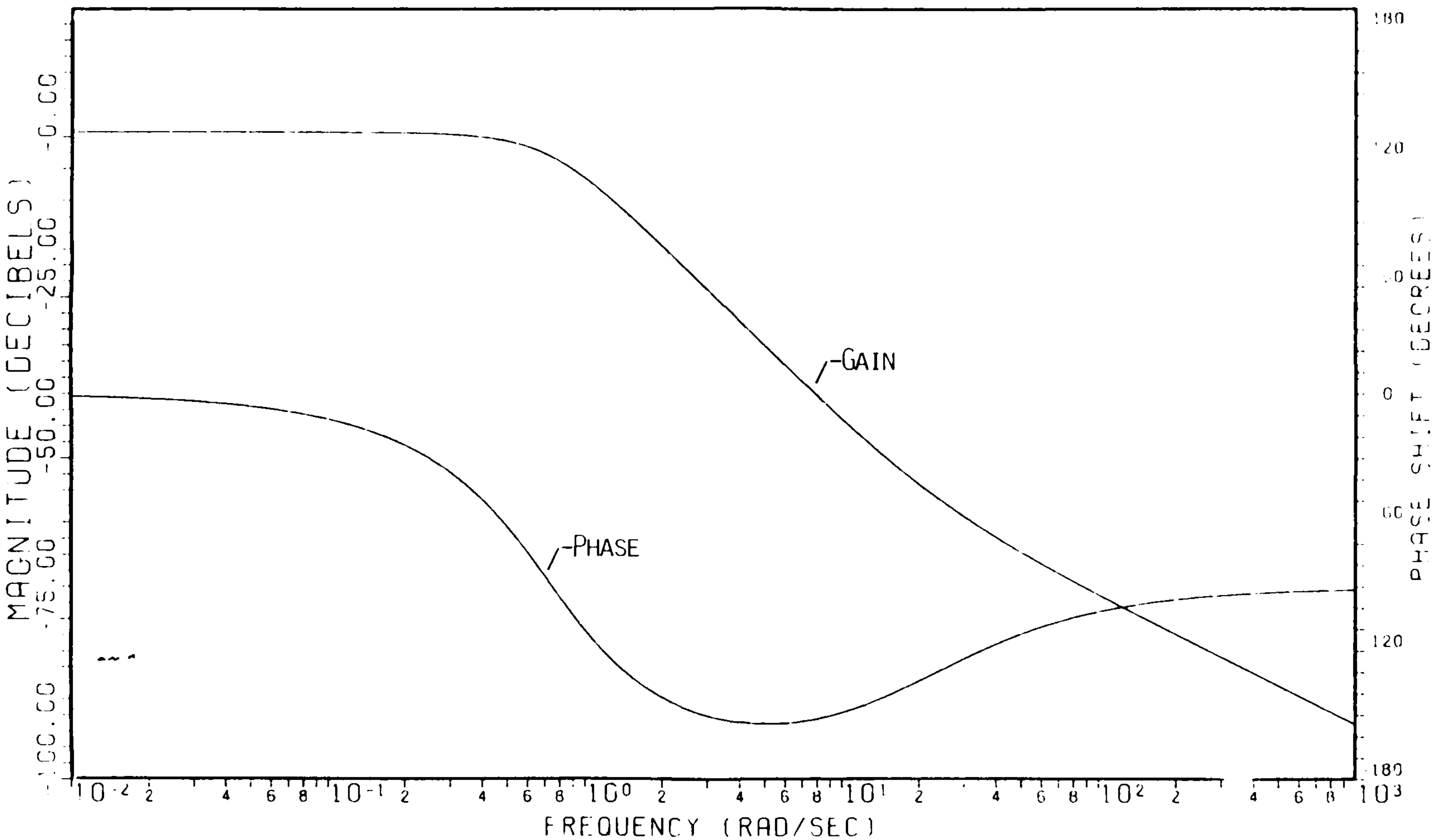

FIGURE 4A OLTF N_2/W_F ROOT LOCUS FOR PLA=40 DEG

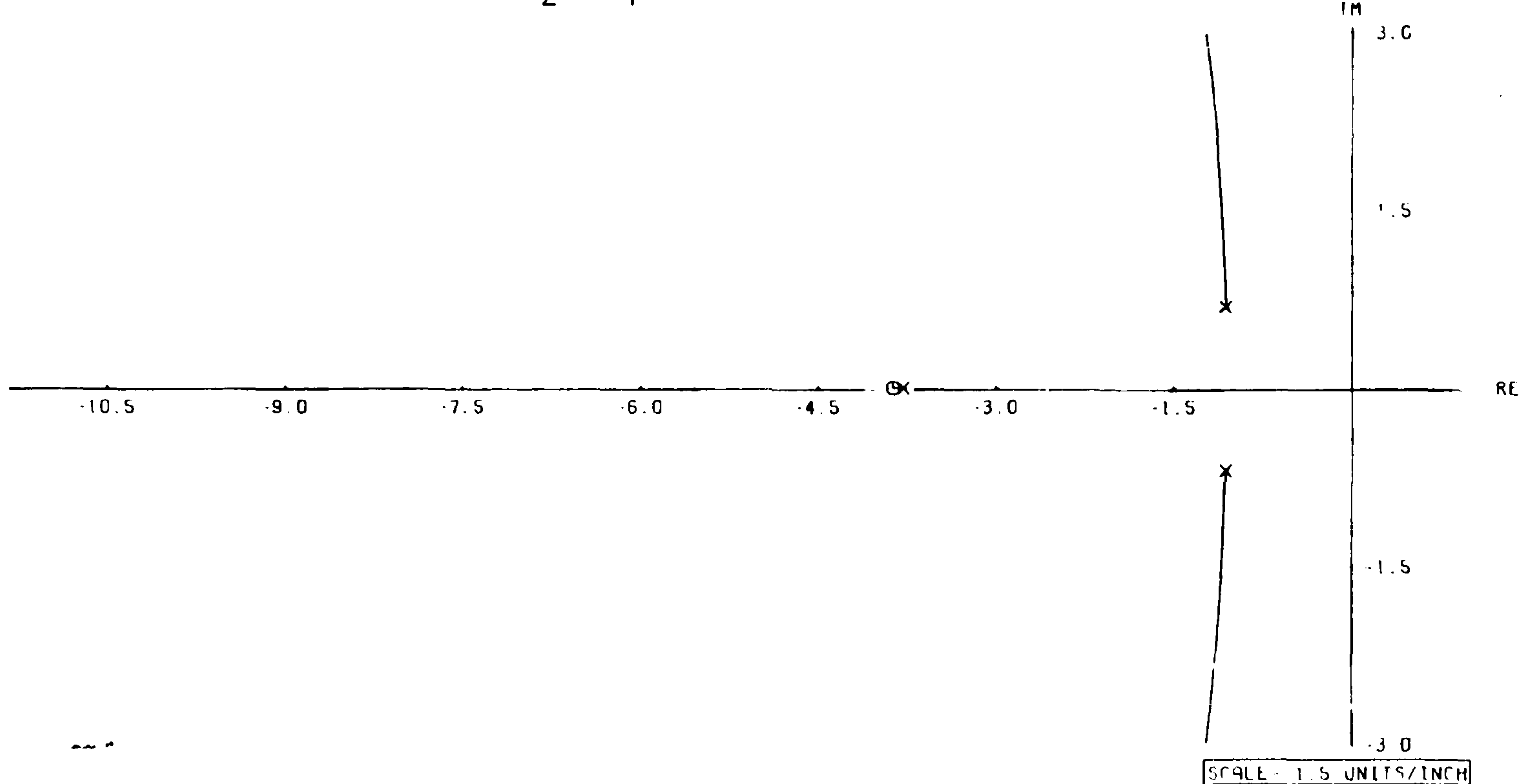

$$OLTF(S) = \frac{K(S+3.868)(S+23.443)}{(S+3.781)(S^2+2.128S+1.609)}$$

FIGURE 4B OLTF N_2/W_F BODE PLOT FOR PLA=40 DEG

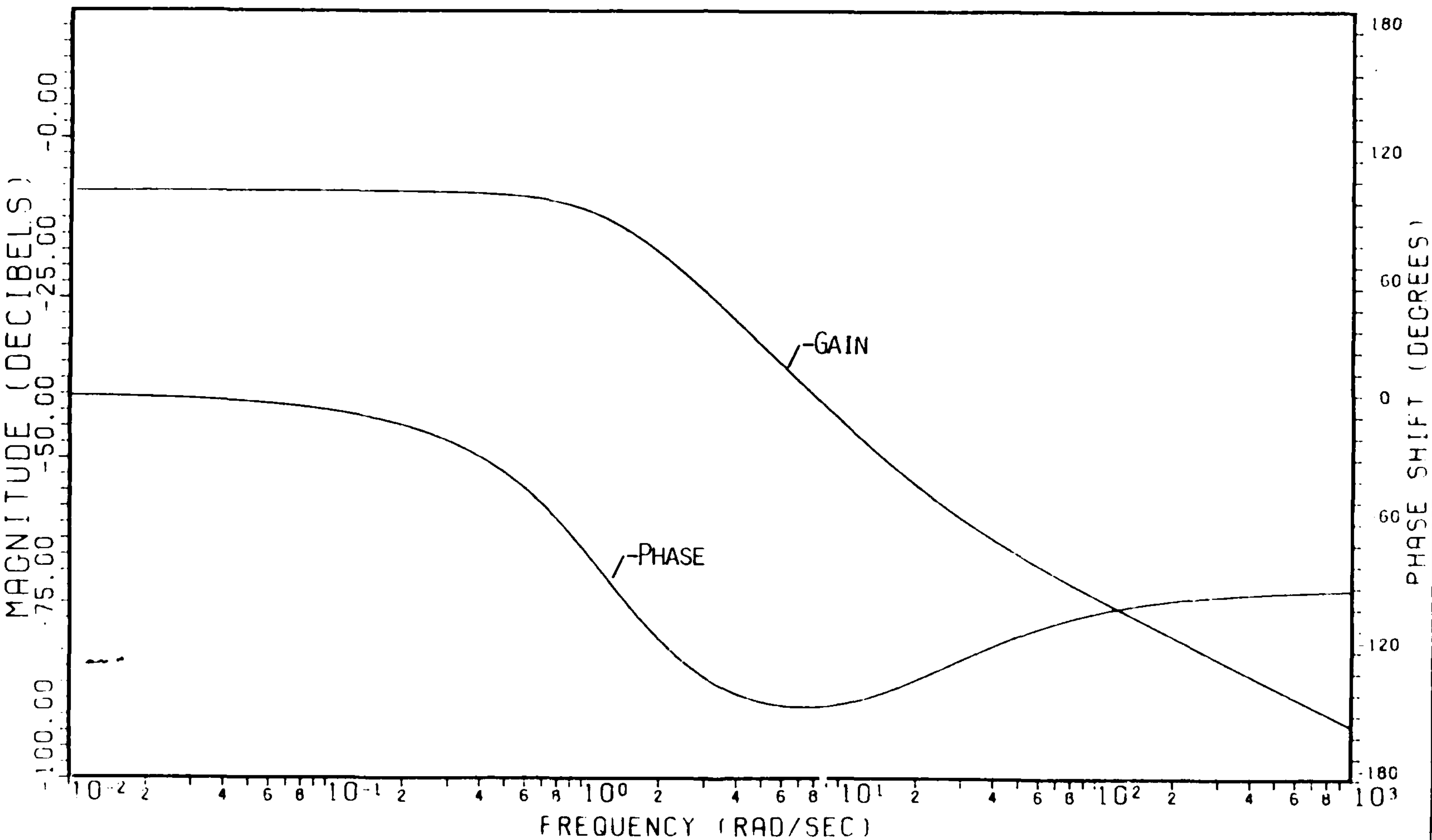

FIGURE 5A OLTF N_2/W_F ROOT LOCUS FOR PLA=45 DEG

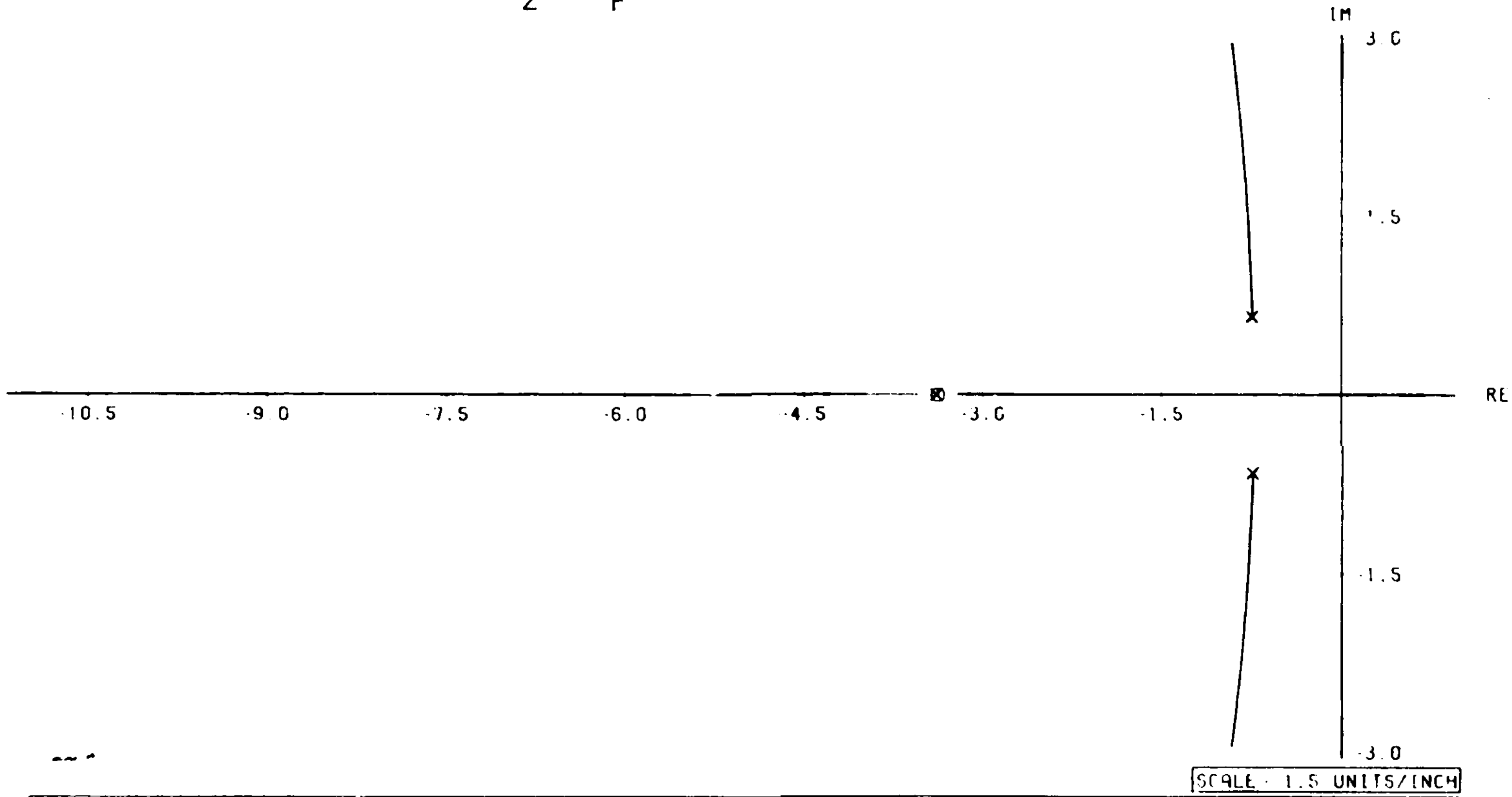

$$OLTF(S) = \frac{K(S+3.379)(S+25.083)}{(S+3.390)(S^2+1.492S+0.988)}$$

FIGURE 5B OLTF N /W BODE PLOT FOR PLA=45 DEG

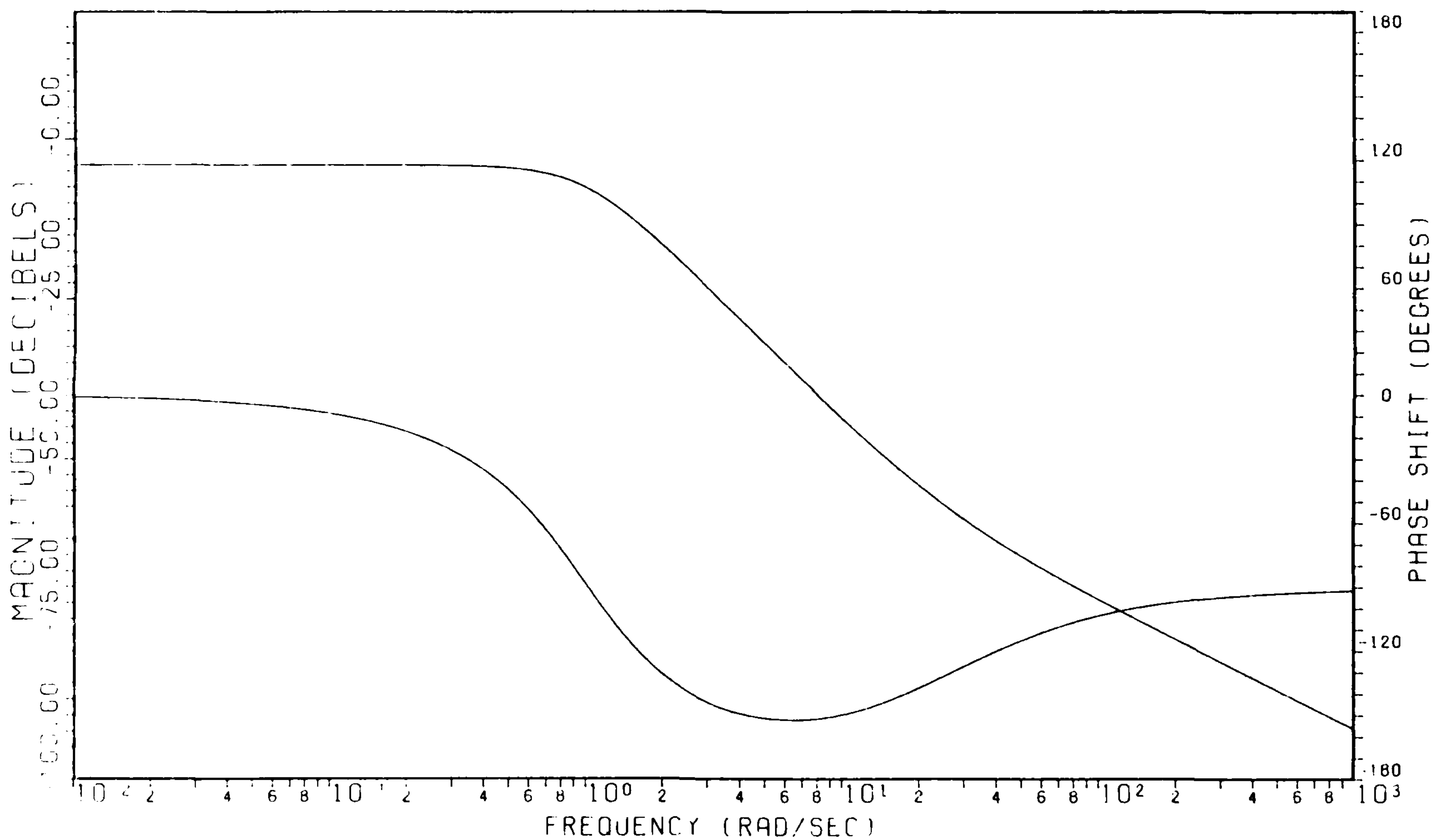

FIGURE 6A OLTF N_2/W_F ROOT LOCUS FOR PLA=50 DEG

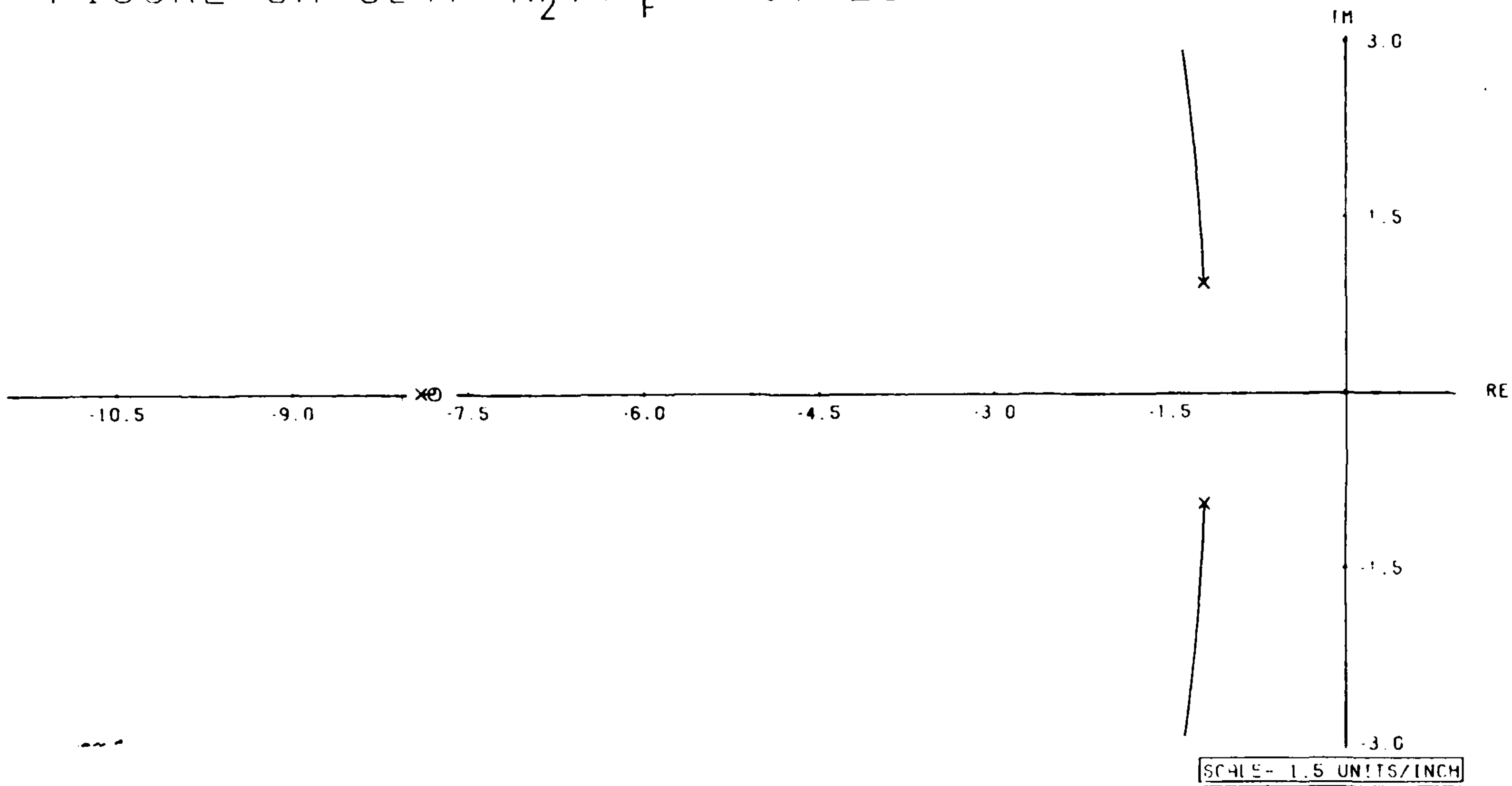

$$OLTF(S) = \frac{K(S+7.785)(S+24.588)}{(S+7.901)(S^2+2.402S+2.336)}$$

FIGURE 6B OLTF N_2/W_F BODE PLOT FOR PLA=50 DEG

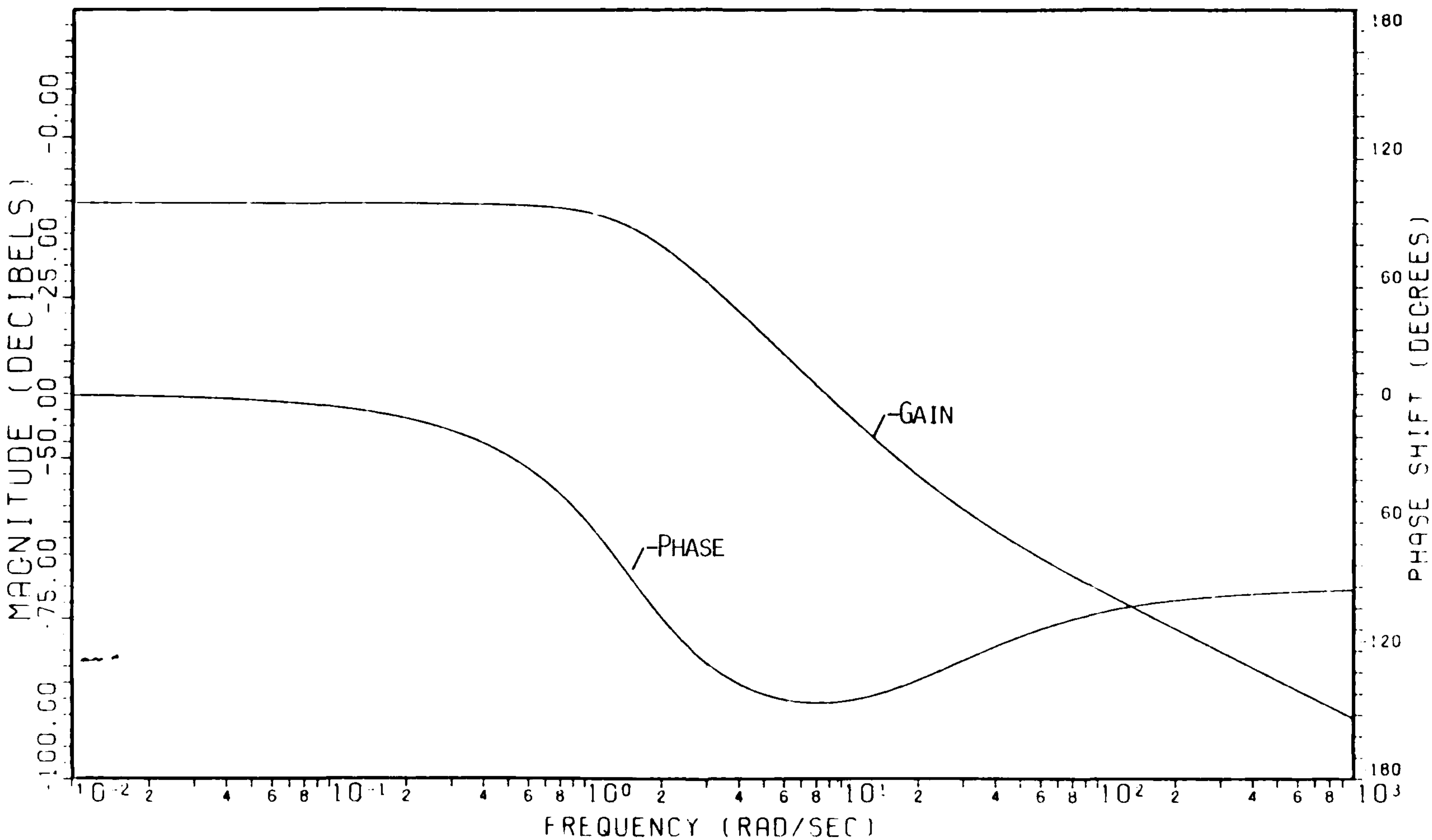

FIGURE 7A OLTF N_2/W_F ROOT LOCUS FOR PLA=55 DEG

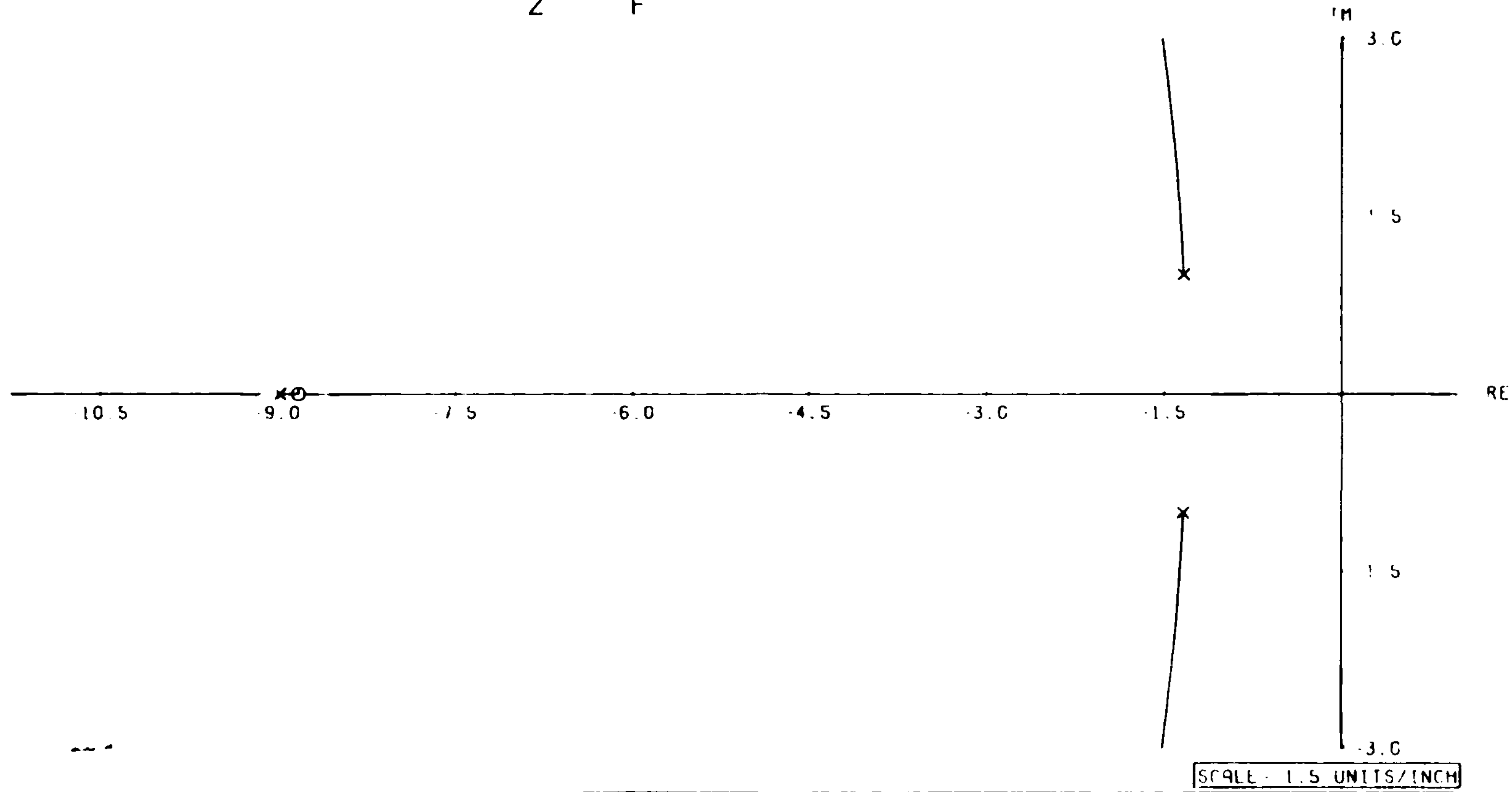

$$OLTF(S) = \frac{K(S+8.831)(S+24.704)}{(S+8.985)(S^2+2.678S+2.809)}$$

FIGURE 7B OLTF N_2/W_F BODE PLOT FOR PLA=55 DEG

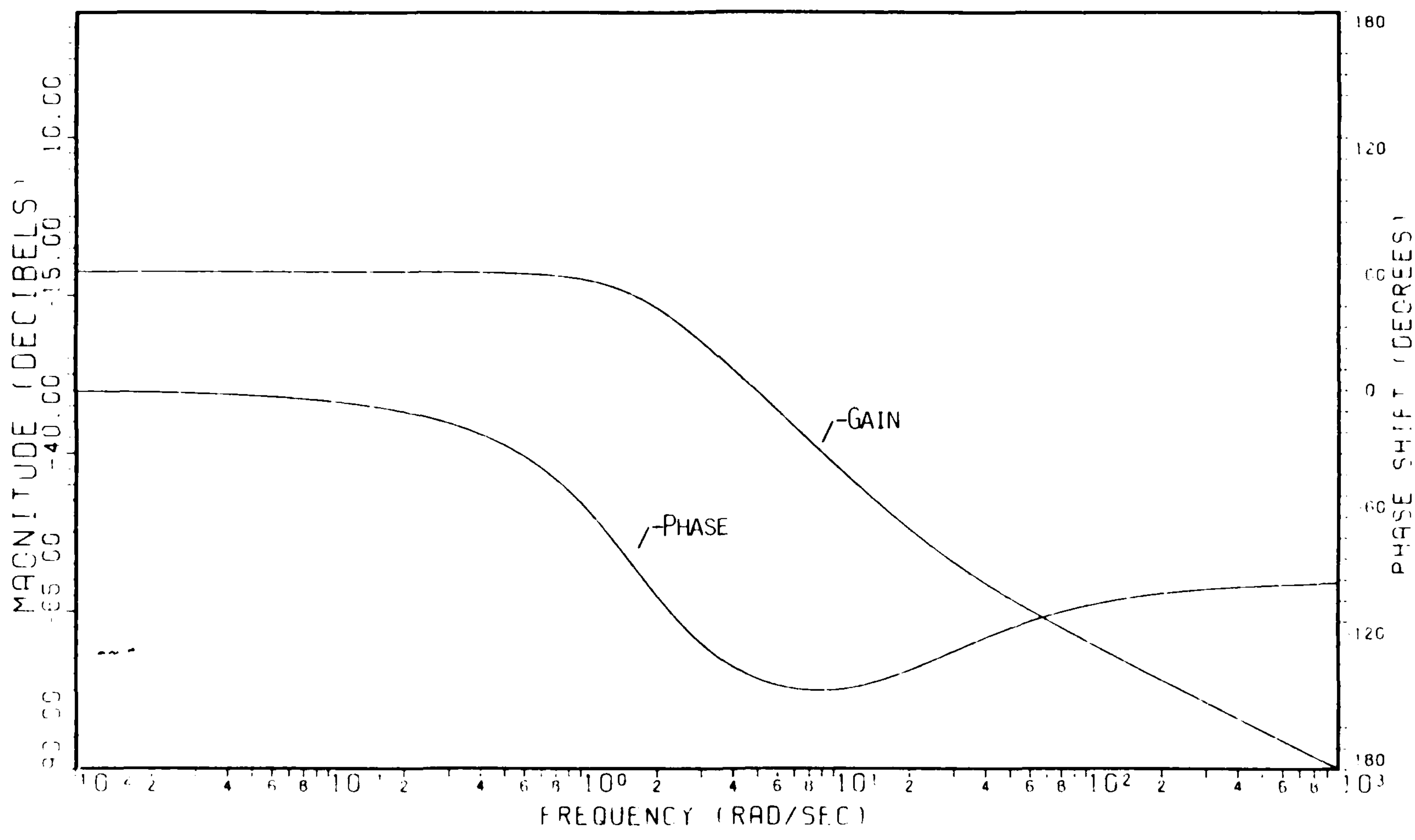

FIGURE 8A OLTF N_2/W_F ROOT LOCUS FOR PLA=60 DEG

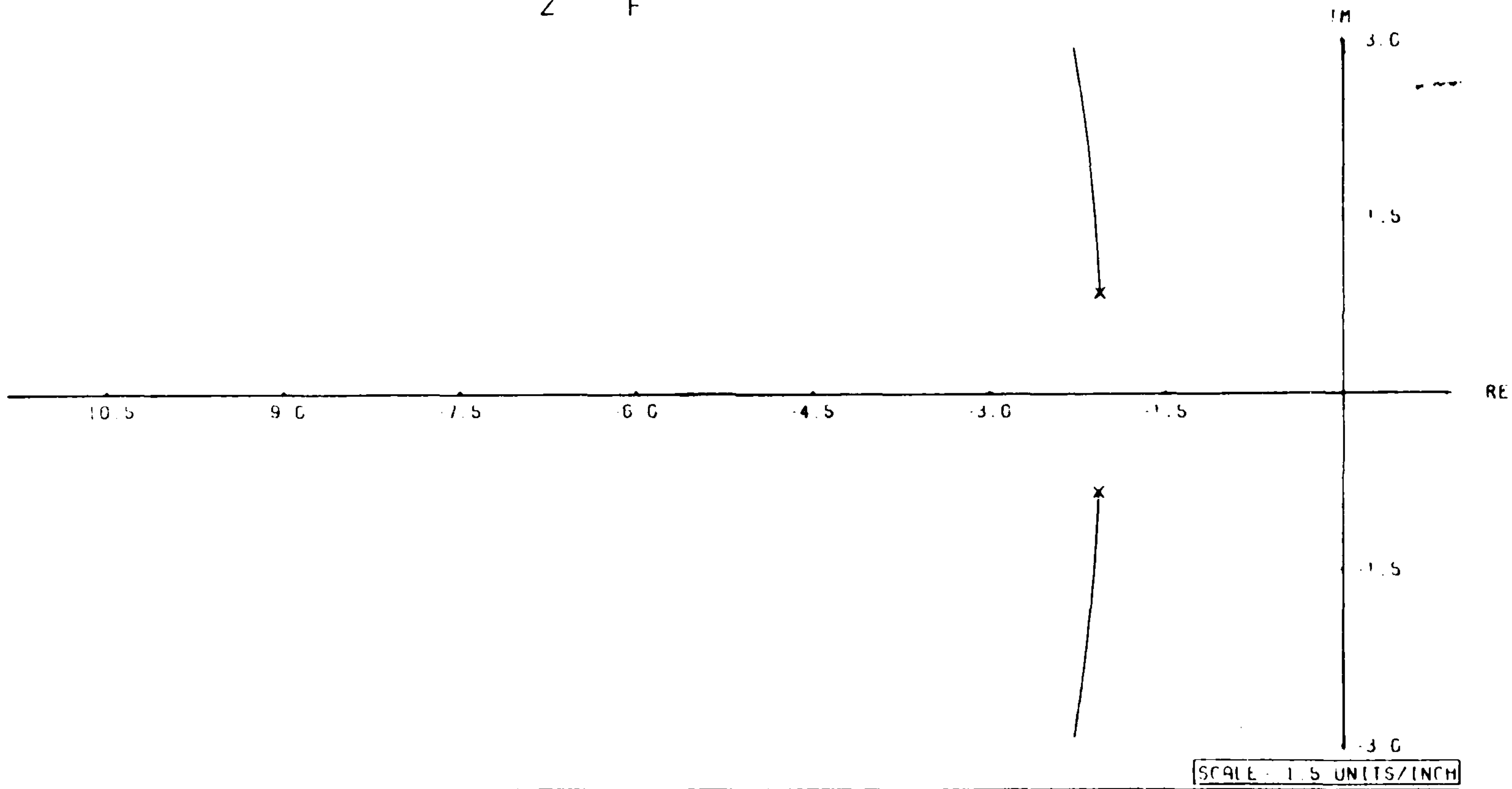

$$OLTF(S) = \frac{K(S+11.144)(S+23.787)}{(S+11.879)(S^2+4.128S+4.978)}$$

FIGURE 8B OLTF N_2/W_F BODE PLOT FOR PLA=60 DEG

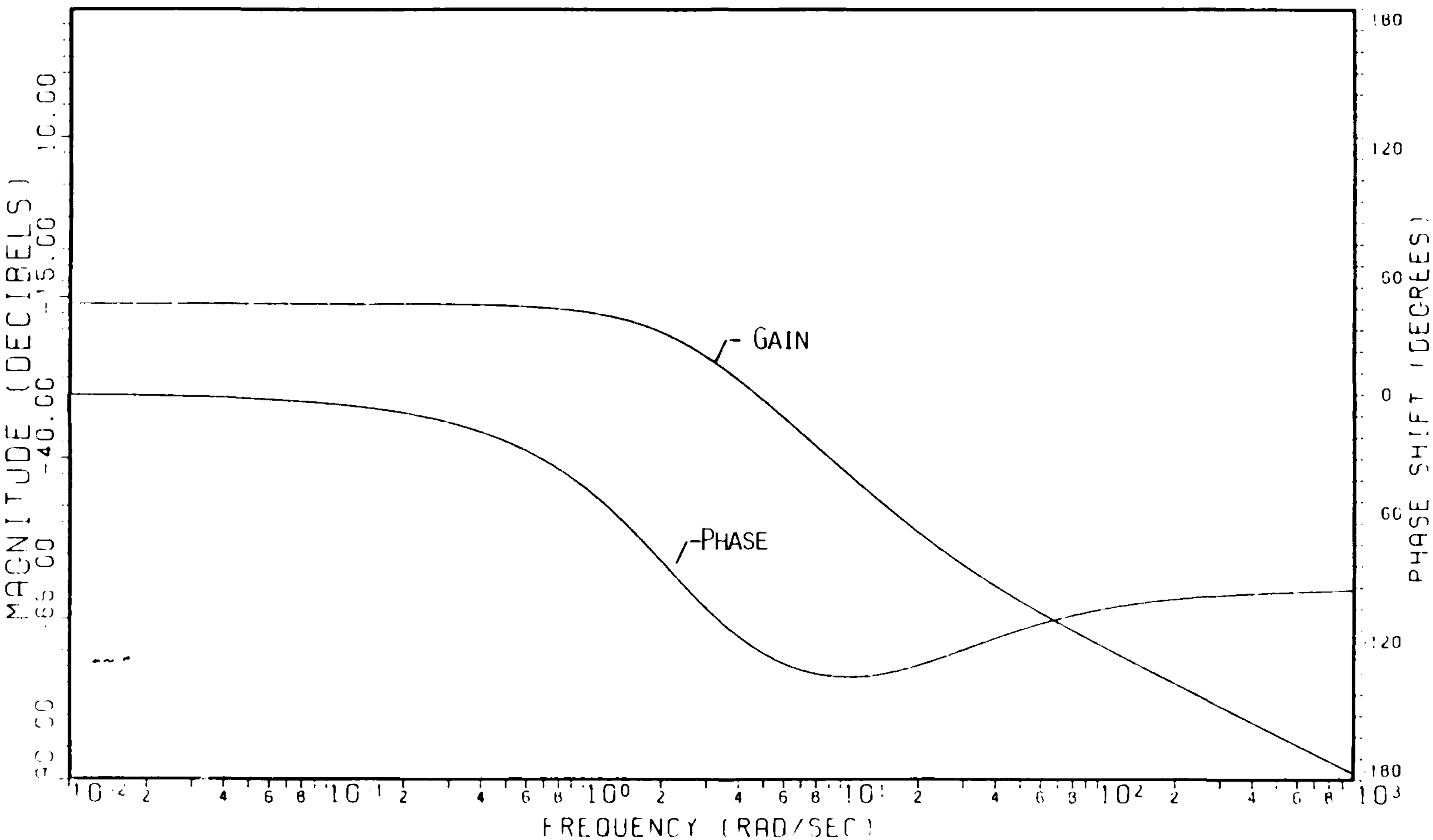

FIGURE 9A OLTF N_2/W_F ROOT LOCUS FOR PLA=65 DEG

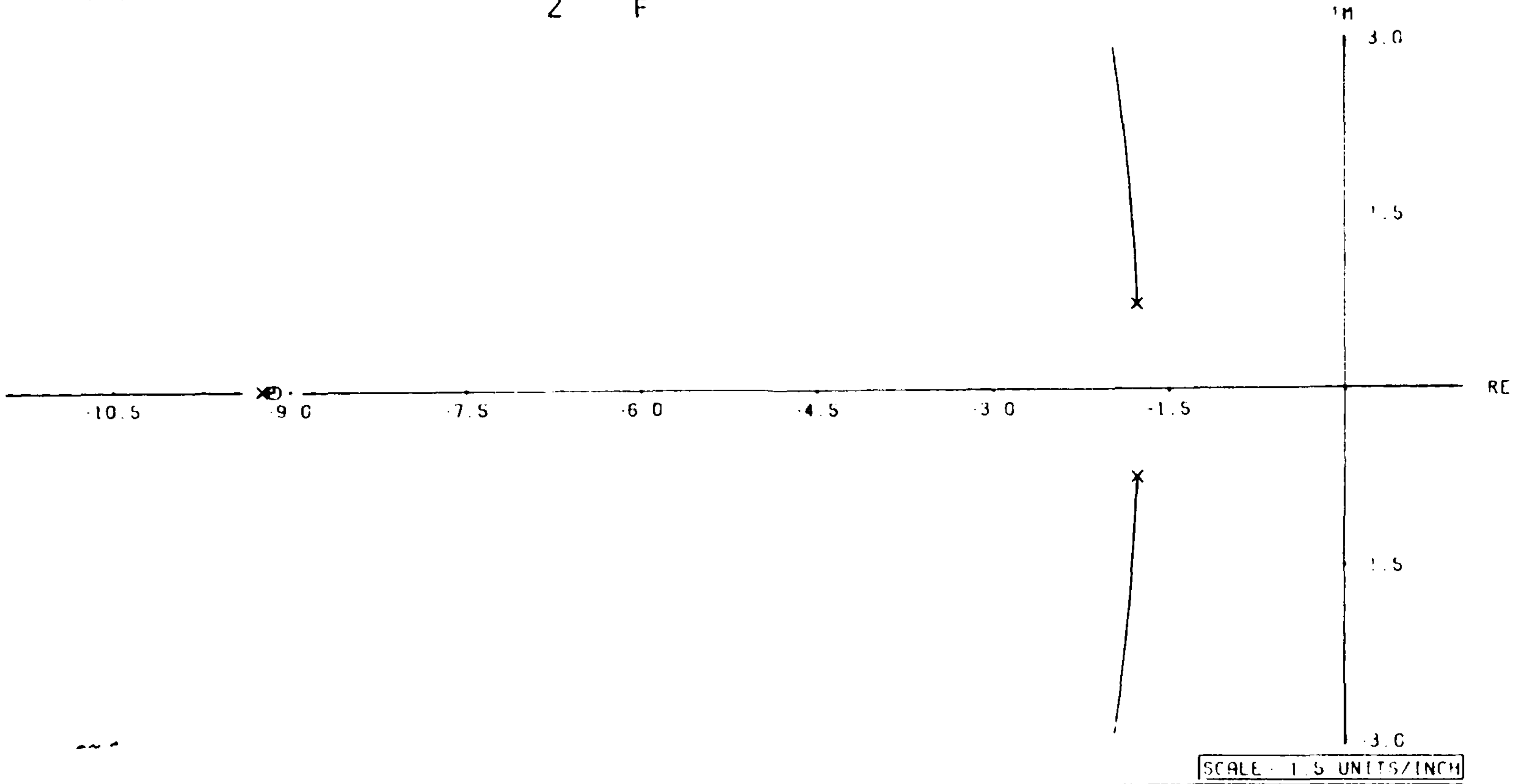

$$OLTF(S) = \frac{K(S+9.140)(S+22.811)}{(S+9.241)(S^2+3.550S+3.695)}$$

FIGURE 9B OLTF N_2/W_F BODE PLOT FOR PLA-65 DEG

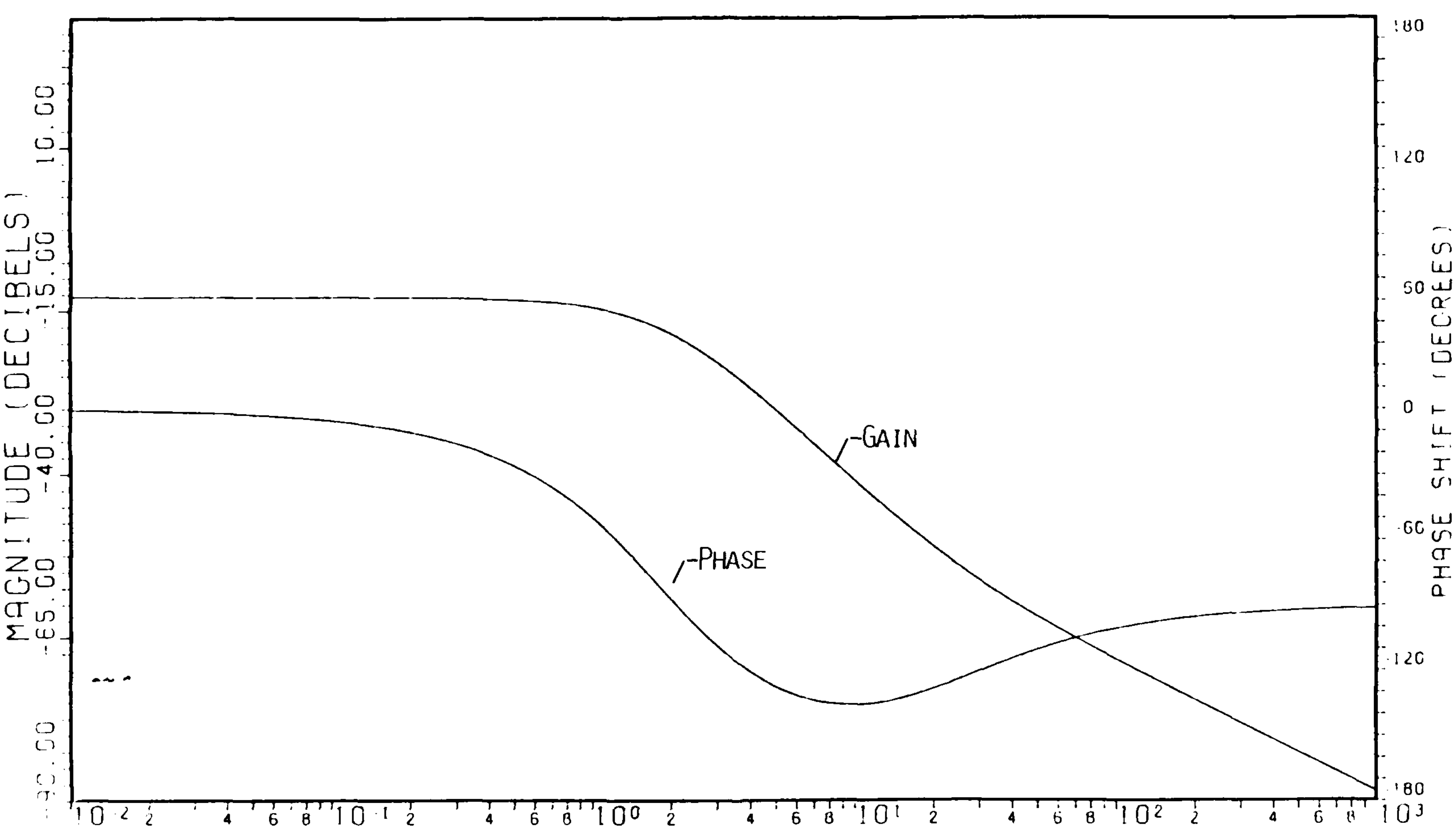

FIGURE 10A OLTF N_2/W_F ROOT LOCUS FOR PLA=70 DEG

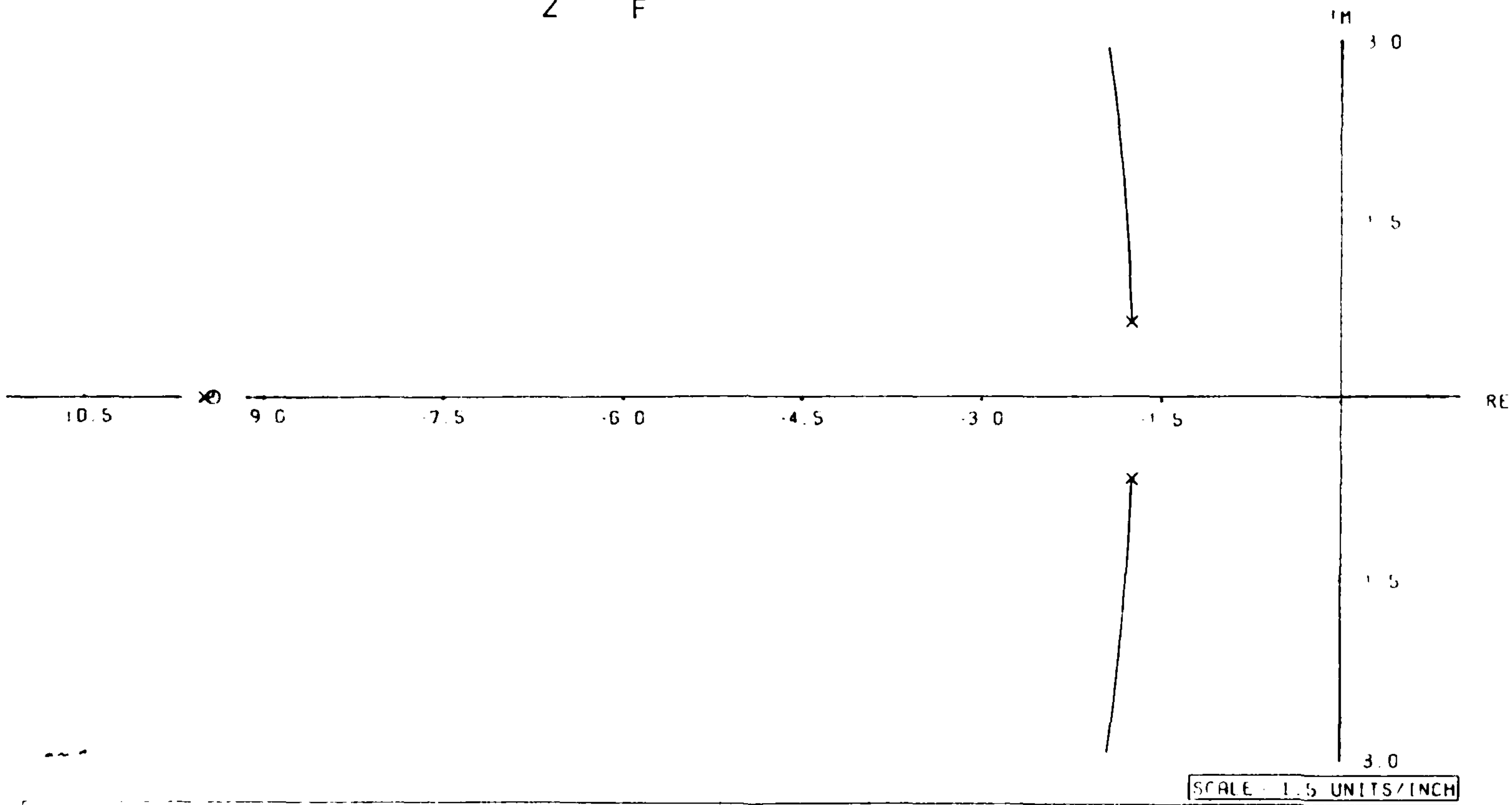

$$OLTF(S) = \frac{K(S+9.423)(S+23.201)}{(S+9.493)(S^2+3.493S+3.477)}$$

FIGURE 10B OLTF N_2/W_F BODE PLOT FOR PLA=70 DEG

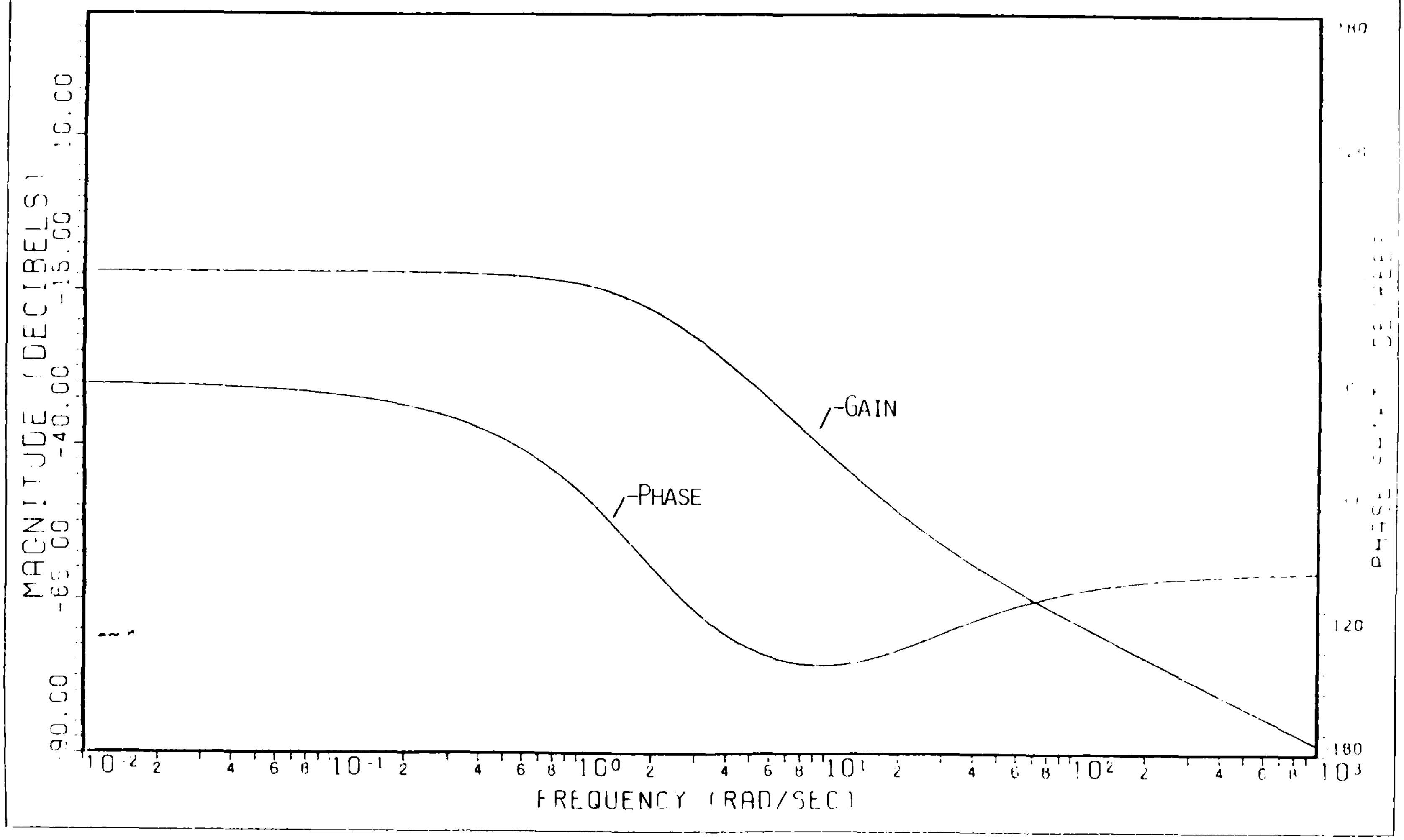

The task of developing a control scheme could now begin, however, at this point in the paper, another means of developing linear thermodynamic state space equations would be of interest and will later be shown to give insight into the make up of the elements of the state space matrices in terms of temperatures, pressures, areas, air and fuel flows.

IV Analytic Equations

Analytic equations describing the thermodynamics of a turbofan engine have been derived[2]. The equations were non-linear, and in all cases failed to tie all components of the engine together.

Recently, however, in a technical report from General Electric's Advanced Engineering Technology Department[3] an attempt was made at deriving linear thermodynamic relationships that encompass all stages of a turbofan engine. Although the equations were not in linear state variable format, they did give linear relationships for crossing various engine stages, the main stages being the low pressure fan (LPF), the high pressure compressor (HPC), the combustor, the high pressure turbine (HPT) and the low pressure turbine (LPT).

To check the accuracies of the linear analytic equations, the F101 engine cycle deck model was used. Values obtained using the linear equations were compared to values obtained using the non-linear cycle deck over small fuel step inputs corresponding to approximately 2 degrees PLA.

Also, the equations derived below will not be identical to those derived in the General Electric report. In some cases, shorter versions of the equations were found to be less complicated yet described the dynamics with greater accuracy. It is important to note again, that the partials derived by General Electric are not in linear state variable format. The analytic equations derived below will keep linear state variable format intact.

Analytic Equation Derivations

When describing the internal mass flow rates and thermodynamic

properties of a turbofan engine, the following equations describing mass flow rates, pressure, and temperature relationships are used extensively:

Flow Function

$$N = \frac{W\sqrt{T}}{AP} \qquad \text{(I)}$$

where,

W = Mass Flow Rate   T = Temperature   A = Area   P = Pressure

N = Restriction Factor (constant when flow is choked),

or in terms of Mach number,

$$N = .766\sqrt{\gamma}\, M\left[1+\frac{(\gamma-1)}{2}\right]^{\frac{\gamma+1}{2(1-\gamma)}} \cong M(2-M) \qquad \text{(II)}$$

Pressure - Temperature Relationship

$$\left(\frac{P_2}{P_1}\right)^{\frac{\gamma-1}{\gamma\eta}} = \frac{T_2}{T_1} \qquad \text{(III)}$$

for adiabatic flow across the LPF, HPC, HPT, or LPT where γ is the ratio of specific heats and η is the adiabatic efficiency.

Static Pressure (P_s) - Mach Number Relationship

$$P_s = P\left(1+\frac{\gamma-1}{2}M^2\right)^{\frac{\gamma-1}{\gamma}} \qquad \text{(IV)}$$

These equations link the various engine components together in non-linear relationships. To linearize each of these equations, the same basic approach of logarithmic derivatives is used.

For the expression

$$A = B*C,$$

the log gives,

$$\log A = \log B + \log C,$$

and taking the partial derivative,

$$\frac{\delta A}{A_e} = \frac{\delta B}{B_e} + \frac{\delta C}{C_e}$$

where (e) signifies equilibruim.

For the expression,

$$A = B + C,$$

taking the log/derivative gives,

$$\frac{A_e \delta A}{A_e} = \frac{B_e \delta B}{B_e} + \frac{C_e \delta C}{C_e}$$

Defining $\partial X/X_e$ as ΔX and $d(\partial X/X_e)/dt$ as $\Delta\dot{X}$ for future reference, equations I through IV become,

$$\Delta N = \Delta W + .5*\Delta T - \Delta A - \Delta P \qquad (\hat{I})$$

$$\Delta N \cong [2(1-M)/(2-M)]\Delta M \qquad (I\hat{I})$$

$$[\Delta P_2 - \Delta P_1](\gamma-1)/\gamma = \Delta T_2 - \Delta T_1 \qquad (II\hat{I})$$

$$\Delta P_s \cong \Delta P - \gamma M^2 \Delta M \qquad (I\hat{V})$$

for constant values of γ and adiabatic efficiency, η .

The log/derivative is a useful and accurate means of linearization. The justification for the definition of ΔX is demonstrated below. For the expression

$$\frac{A*B}{\sqrt{C}},$$

small changes about an equilibrium can be definded as

$$A = A_e + \delta A$$
$$B = B_e + \delta B$$
$$C = C_e + \delta C.$$

Substitution gives,

$$\frac{(A_e + \delta A)(B_e + \delta B)}{\sqrt{C_e + \delta C}}.$$

Multiplying through and neglecting second order terms,

$$\frac{A_e B_e + A_e \delta B + B_e \delta A}{\sqrt{C_e}(1 + \delta C / C_e)^{1/2}}.$$

Substitution of the binomial expansion

$$\frac{1}{(1 + \delta C / C_e)^{1/2}} \cong (1 - .5(\delta C / C_e)),$$

and dividing by $A_e B_e \sqrt{C_e}$ gives the final desired solution as,

$$\frac{\delta A}{A_e} = \frac{\delta B}{B_e} - .5\frac{\delta C}{C_e}$$

As stated before, the equations used in this paper differ somewhat from the equations described in the General Electric report (different intended uses) and will be derived below in linear state variable format starting with the engine inlet and ending at the engine nozzle algebraicly connecting each engine stage to the next. Figure 11 describes by number the various engine stages and locations of pressures, temperatures, and mass flow rates used in the derivation of the linear equations and should be referenced as the equations progress from stage to stage.

TURBOFAN ENGINE

FIGURE 11

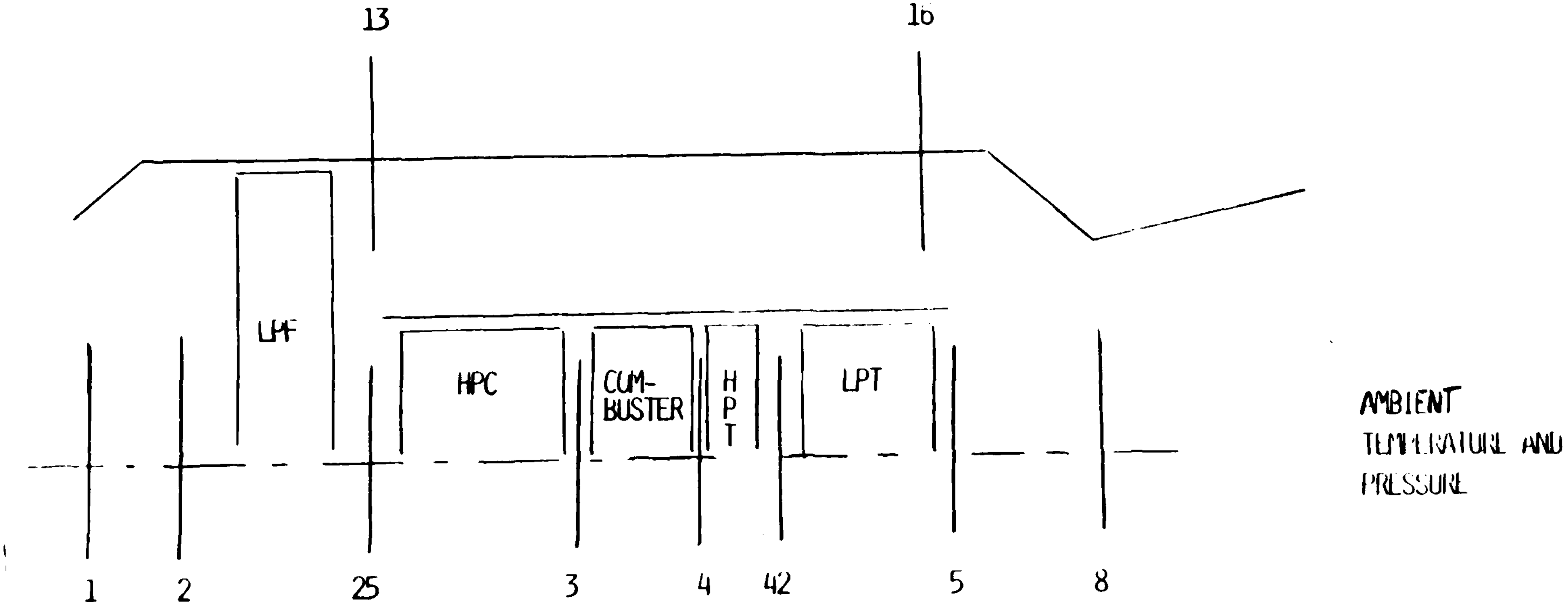

ENGINE STATION DESIGNATION

STATION

1	ENTRANCE TO INLET
2	LPF INLET
13	FORWARD DUCT BYPASS
16	AFT DUCT BYPASS
25	HPC INLET
3	COMBUSTER INLET
4	HPT INLET
42	LPT INLET
5	LPT EXIT
8	NOZZLE AREA

TURBOFAN - A HIGH SPEED SPOOL SURROUNDED BY A LOW SPEED SPOOL

Engine Stages

Engine Inlet

Isentropic flow is assumed in the inlet giving

$T_1 = T_2$
$P_1 = P_2$
$W_1 = W_2$.

Flow across the fan is assumed adiabatic, and the form of Equation (III) states,

$$\left(\frac{P_{13}}{P_2}\right)^{\frac{\gamma_f - 1}{\gamma_f \eta_f}} = \frac{T_{13}}{T_2} \quad \text{for bypass flow, and}$$

$$\left(\frac{P_{25}}{P_2}\right)^{\frac{\gamma_c - 1}{\gamma_c \eta_c}} = \frac{T_{25}}{T_2} \quad \text{for core flow.}$$

Taking the log/partial and assuming a constant γ and efficiency, η in the duct and core, the equations become,

$$\frac{(\gamma_f - 1)}{\gamma_f \eta_f}\left[\Delta P_{13} - \Delta P_2\right] = \Delta T_{13} - \Delta T_2 \qquad \text{(Bypass)}$$

$$\frac{(\gamma_c - 1)}{\gamma_c \eta_c}\left[\Delta P_{25} - \Delta P_2\right] = \Delta T_{25} - \Delta T_2 \qquad \text{(Core).}$$

If the flight Mach number is held constant, ΔT_2 and ΔP_2 will be zero. To further simplify the derivation of these and further equations, the expression $(\gamma - 1)/\gamma$, will be defined as

GNFD for the fan bypass flow
GNF for the fan core flow
GNC for the compressor core flow
GNT for the turbine core flow

The above equation for duct bypass flow and compressor flow are now written as,

$$\Delta P_{13} = (GNFD)\Delta T_{13} \qquad \text{(Duct Flow)}$$

$$\Delta P_{25} = (GNF)\Delta T_{25} \qquad \text{(Compressor Flow)} \tag{2}$$

<u>Fan Duct Flow</u>

The flow function within the duct follows Equation $(\hat{I})$ and gives,

$$\Delta N_{13} = \Delta WB + .5\Delta T_{13} - \Delta P_{13} \tag{3a}$$

If no losses are assumed through the duct,

$$\begin{aligned} \Delta T_{13} &= \Delta T_{16} \\ \Delta P_{13} &= \Delta P_{16} \\ \Delta N_{13} &= \Delta N_{16} \end{aligned} \tag{3b}$$

<u>Compressor Flow</u>

Flow across the compressor is assumed adiabatic satsifying Equation $(I\hat{I}I)$ to give

$$\Delta T_3 = \Delta T_{25} + \Delta P_3/GNC - \Delta P_{25}/GNC \tag{4}$$

<u>Engine Combuster</u>

The equation governing the flow and heat gain in the combustor is

$$W_{25}(h_{39} - h_3) = W_f(LHV) \tag{5}$$

where,

W_{25} = air flow in core
h = enthapy at specified engine location (equal to Cp*T)
W_f = fuel flow
LHV = lower heating value of fuel (assumed constant)
T_{39} = turbine inlet temperature prior to turbine rotor heat soak

The turbine rotor on the F101 engine is very massive and the temperature heat soak dynamics play a sizable part in determining engine dynamcs.

Taking the log/derivative gives

$$\Delta W_f = \Delta W_{25} + \Delta T_{39}(Z_4/(Z_4-1)) - \Delta T_3/(Z_4-1) \qquad (5a)$$

where $Z_4 = T_{39}/T_3$.

Across the combustor, the pressure drop is assumed small enough and the pressure ratio P_4/P_3 nearly constant such that,

$$\Delta P_3 = \Delta P_4 \qquad (5b)$$

The accuracy of this assumption will be discussed in the error analysis section.

Turbine Inlet

Flow into the turbine inlet is assumed choked. This may not, however, be the case at near idle conditons, but using the cycle deck model, the restriction factors could be computed at the low idle speeds. For the majority of engine operations,

$$\frac{W_{25}\sqrt{T_{25}}}{A_{41}P_{41}} = \text{Constant}$$

or,

$$\Delta P_4 = \Delta W_{25} + .5\Delta T_4. \qquad (6)$$

where ΔT_4 has been previously defined in the empirical equation discussion as TIT. TIT and T_4 can be used interchangeably.

High Pressure Turbine

The assumption made for flow across the high pressure turbine is

$$\Delta T_4 = \Delta T_{42}$$

This is a reasonably accurate assumption and will be discussed later during the error analysis section.

Low Pressure Turbine

As before, adiabatic flow across the low pressure turbine is assumed. The appropriate equation is,

$$\left(\frac{P_5}{P_{42}}\right)^{\frac{\gamma-1}{\gamma\eta}} = \frac{T_5}{T_{42}}$$

which gives,

$$\Delta P_5 = \Delta P_{42} + (\Delta T_5 - \Delta T_4)/GNT. \qquad (7a)$$

The equation for the restriction factor,

$$N_5 = \frac{W_5\sqrt{T_5}}{A_5 P_5}$$

gives,

$$\Delta N_5 = \Delta W_{25} + .5\Delta T_5 - \Delta P_5 \qquad (7b)$$

Unbalanced Power

Fan

The horsepower of the fan, (FP), is given by definition as,

$$FP = (T_{13} - T_2)W_2,$$

or after the log/derivative,

$$\Delta FP = \Delta W_2 + \Delta T_{13} Z_6 \qquad (8)$$

where, $Z_6 = T_{13}/(T_{13}-T_2)$.

Low Pressure Turbine (LPT)

The horsepower of the low pressure turbine, (LP), is given by definition as,

$$LP = (T_5 - T_{42})W_{25}, \text{ which produces,}$$

$$LP = \Delta W_{25} + \Delta T_{42}Z_9 + \Delta T_5(1-Z_9) \qquad (9)$$

where, $Z_9 = T_{42}/(T_{42}-T_5)$

The difference between the fan horsepower and the LPT horsepower would be zero in equilibrium. However, when not in equilibrium, the differences are equal to the off-torque, $I_{N1}\dot{N}_1$, where I_{N1} is the low pressure spool inertia. In log/derivative format,

$$\begin{aligned}\Delta\dot{N}_1 &= \Delta LP - \Delta FP\\ &= \Delta W_{25} + \Delta T_4 Z_9 + \Delta T_5(1-Z_9) - \Delta W_2 + \Delta T_{13}. \qquad (10)\end{aligned}$$

Compressor

In a similar manner to the LPF and the LPT, the compressor horsepower, CP, log/differential is,

$$\Delta CP = \Delta W_{25} + \Delta T_3 Z_7 + \Delta T_{25}\ (1+Z_7) \qquad (11)$$

where, $Z_7 = T_3/(T_3-T_{25})$.

High Pressure Turbine (HPT)

The equations governing the HPT are

$$HP = (T_{42} - T_4)W_{25} \text{ and,}$$

$$\Delta HP = \Delta W_{25} + \Delta T_4 \qquad (12)$$

remembering that $\Delta T_{42} = \Delta T_4$.

The difference in the torque for the HPT and compressor gives the off-torque for the high speed rotor as,

$$\Delta HP - \Delta CP = \Delta T_4 - \Delta T_3 Z_7 - \Delta T_{25}(1-Z_7). \qquad (13)$$

Using Equations (2), (4), (5b), and (6), the ΔT_3 term can be rewritten as,

$$\Delta T_3 = \Delta T_{25}(1 - GNFD/GNC) + W_{25}/GNC + T_4/(2(GNC)) \qquad (14)$$

Substitution of Equation (14) into Equation (13) gives,

$$\Delta \dot{N}_2 = \Delta HP - \Delta CP$$

$$= -\Delta W_{25} Z_7/GNC + \Delta T_4(1 - Z_7/(2(GNC)) + \Delta T_{25}(Z_7(GNFD/GNC) -1). \qquad (15)$$

Temperature Heat Soak

In equilibrium, T_{39} is equal to T_4 since the HPT rotor is in thermal equilibrium. When fuel is added, T_{39} immediately rises. However, T_4 takes some finite amount of time to regain thermal equilibrium. The differential equation which describes the turbine rotor thermal dynamics due to fuel flow input is

$$\dot{T}_4 = K_4 Z_3 (T_{39})$$

where T_{39} has already been shown a function of W_{25}, T_4, T_{25} and W_f. Taking the log/derivative, the equation becomes,

$$\Delta \dot{T}_4 = K_4(\Delta T_{39} Z_3) \qquad (16)$$

where K_4 is the heat soak time constant and $Z_3 = T_{39}/T_4$. Using the expression for ΔT_{39} from Equation (5a) and substitution of Equation (14) into Equation (16) gives,

$$\Delta \dot{T}_4/K_4 = (Z_4/Z_4)[\Delta W_{25}((1 - Z_4) + 1/GNC) + \Delta T_4/(2(GNC)) +$$
$$\Delta T_{25}(1\text{-}GNFD/GNC) + \Delta W_f(Z_4 - 1)] \qquad (17)$$

Equations (10), (15), and (17) make up a partial state space matrix of the form,

$$[\dot{X}] = [A][W] + [B][U] + [E][V],$$

or in terms of engine parameters,

$$\frac{d}{dt}\begin{bmatrix} \Delta N_1 \\ \Delta N_2 \\ \Delta T_4/k_4 \end{bmatrix} = [A]\begin{bmatrix} \Delta W_2 \\ \Delta W_{25} \\ \Delta T_4 \end{bmatrix} + [B]\begin{bmatrix} \Delta W_f \\ \Delta A_8 \end{bmatrix} + [E]\begin{bmatrix} \Delta T_{13} \\ \Delta T_5 \\ \Delta T_{25} \end{bmatrix} \qquad (18)$$

where,

$$[A] = \begin{bmatrix} -1 & 1 & Z_9 \\ 0 & -Z_7/GNC & (1-Z_7)/(2(GNC)) \\ 0 & Z_3/Z_4(1/GNC+(1-Z_4) & 1/(2(GNC)) \end{bmatrix},$$

$$[B] = \begin{bmatrix} 0 & 0 \\ 0 & 0 \\ (Z_4-1) & 0 \end{bmatrix}, \quad [E] = \begin{bmatrix} 0 & (1-Z_9) & \bullet \\ 0 & 0 & Z_7(GNFD/GNC)-1 \\ 0 & 0 & (1-GNFD/GNC) \end{bmatrix}.$$

Continuity Equations

To transform the above equation into the conventional form,

$$[\dot{X}] = [A][X] + [B][U],$$

the continuity equations for a turbofan engine are employed.

The total nozzle area for the F101 is made up of the bypass duct area, A_{8B}, and the core area A_{8C}. Remembering the restriction factor in the duct, N is

$$N_{13} = \frac{W_{13}\sqrt{T_{13}}}{A_{13}P_{13}} . \qquad (19)$$

continuity of flow at station 8 (the nozzle) gives,

$$\frac{N_{13}A_{13}P_{13}}{\sqrt{T_{13}}} = \frac{N_8 A_{8C} P_8}{\sqrt{T_8}}$$

Taking the log/derivative and recalling ΔA13 is zero,

$$\Delta A_{8B} = \Delta N_{13} + .5\Delta T_8 - .5\Delta T_{13} - \Delta P_8 + \Delta P_{13}. \qquad (20)$$

Flow at station 5, the LPT outlet, must also satisfy continuity. The relationship gives,

$$\Delta A_{8C} = \Delta N_5 + .5\Delta T_8 - .5\Delta T_5 - \Delta P_8 + \Delta P_5. \qquad (21)$$

As stated earlier, the nozzle area is made up of both core and bypass area such that $A_8 = A_{8B} + A_{8C}$, or after the log/derivative,

$$A_8\Delta A_8 = A_{8B}\Delta A_{8B} + A_{8C}\Delta A_{8C} . \qquad (22a)$$

Each area satisfies the following,

$$A_8 = \frac{(W_{13} + W_{25}\sqrt{T_8})}{P_8} \qquad (22b)$$

$$A_{8B} = \frac{W_{13}\sqrt{T_8}}{P_8} \qquad (22c)$$

$$A_{8C} = \frac{W_{25}\sqrt{T_8}}{P_8} \ . \qquad (22d)$$

Dividing Equation (22b) by (22d) gives,

$$\Delta A_8 (1 + B) = \Delta A_{8B} B + \Delta A_{8C} \ . \qquad (23)$$

where B is the air flow bypass ratio W_{13}/W_{25}. Substitution of Equations (20) and (21) into Equation (23) gives,

$$\Delta A_8 (1 + B) = \Delta N_{13} B + .5\Delta T_8 B - .5\Delta T_{13} B - \Delta P_8 B + \Delta P_{13} B + \Delta N_5 + .5\Delta T_8 - .5\Delta T_5 - \Delta P_8 + \Delta P_5 \ . \qquad (24)$$

When two seperate air flows mix, in this case the duct bypass and core air flows, an approximation of the final temperature state is a flow weighting of the two air flows. At station 8, the mixing point, the equation for temperature is,

$$(W_{25} + W_{13})T_8 = W_{13}T_{13} + W_{25}T_5 .$$

Rewriting in terms of constant bypass ratio, B, and taking the log/derivative,

$$\Delta T_8 (1 + Q) = \Delta T_{13} + \Delta T_5 \ , \qquad (25a)$$

where $Q = B(T_{13}/T_5)$.

A simplified means of mixing pressures P_{13} and P_5 based on experimental results of tested turbofan engine data gives the log/derivative relationship,

$$\Delta P_8(1 + B) = \Delta P_{13}B + \Delta P_5. \qquad (25b)$$

Accuracies of the assumptions made in Equations (25a) and (25b) will be considered in the discusion on error analysis. Substituting Equations (25a) and (25b) into Equation (24) results in,

$$\Delta A_8(1 + B) = \Delta N_{13}B + \Delta N_5 + .5\Delta T_5 Z_5 - .5\Delta T_{13} Z_5. \qquad (26)$$

where $Z_5 = (B - Q)/(1 + Q)$.

Substitution of Equations (7a) and (7b) into Equation (6) defines the restriction factor at station 5 as

$$\Delta N_5 = \Delta T_4 (1/GNT - 1/2) - \Delta T_5 (1/GNT - 1/2). \qquad (27)$$

Further substitution of Equations (2), (3b), and (27) into Equation (26) gives the first continuity equation in final form being,

$$\Delta A_8(1 + B) = \Delta W_2 (1 + B) - \Delta W_{25} + \Delta T_4 (1/GNT - 1/2) + \Delta T_{12} (B/2 - B(GNF) - Z_5/2) + \Delta T_5 (Z_5/2 - 1/GNT + 1/2) \qquad (28)$$

Another continuity conditon must also be satisfied. When the duct and core mass air flows mix, the static prssures at the mixing point must be equal, or for the F101 engine,

$$P_{s16} = P_{s5}.$$

Recalling that there are no losses, P_{s16} is also equal to P_{s13} just as P_{16} is equal to P_{13}. These terms will be used interchangable.

The relationship between restriction factor and Mach number, M, is given by,

$$N_{16} = 766\sqrt{\gamma_{16}}\, M_{16}\left[1 + \frac{(\gamma_{16} - 1)}{2} M_{16}^2\right]^{\frac{\gamma_{16} + 1}{2(1 - \gamma_{16})}} \qquad (29)$$

This equation becomes very cumbersome when taking the log/derivative.

Based on past General Electric performance data from turbofan engine testing, a simplified equaton for the restriction factor over the operational range of an engine is,

$$N_{16} \cong M_{16}(2 - M_{16}) \qquad (30)$$

The accuracy of this equation relative to Equation (29) can be seen in Figure 12 which plots Equation (30) versus Equation (29) as a function of Mach number. The relationship between static and total pressures as a function of Mach number is by definition,

$$\frac{P_{16}}{P_{s16}} = \left[1 + \frac{\gamma_{16} - 1}{2} M_{16}^2\right]^{\frac{\gamma_{16}}{\gamma_{16} - 1}} . \qquad (31a)$$

Taking the log of both sides, and using the log series approximation, Equation (31a) becomes,

$$\log P_{s16} \cong \log P_{16} - .5\gamma_{16} M_{16}^2 \qquad (31b)$$

Considering station 16 and taking the log/derivative, Equations (30), and (31b) yield,

$$\Delta N_{16} = \Delta M_{16}[2(1 - M_{16})/(2 - M_{16})] \qquad (32a)$$

$$\Delta P_{s16} = \Delta P_{16} - \gamma_{16} M_{16}^2 \Delta M_{16} \qquad (32b)$$

Combining Equations (32a) and (32b) gives the desired result in terms of static pressure as

$$\Delta P_{s16} = \Delta P_{13} - \Delta N_{16} Z_1 \qquad (32c)$$

where P_{13} is substituted for P_{16} and $Z_1 = \gamma M_{16}^2/2(2 - M_{16})/(1 - M_{16})$.

Similarly for station 5,

$$\Delta P_{s5} = \Delta P_5 - \Delta N_5 Z_2 . \qquad (32d)$$

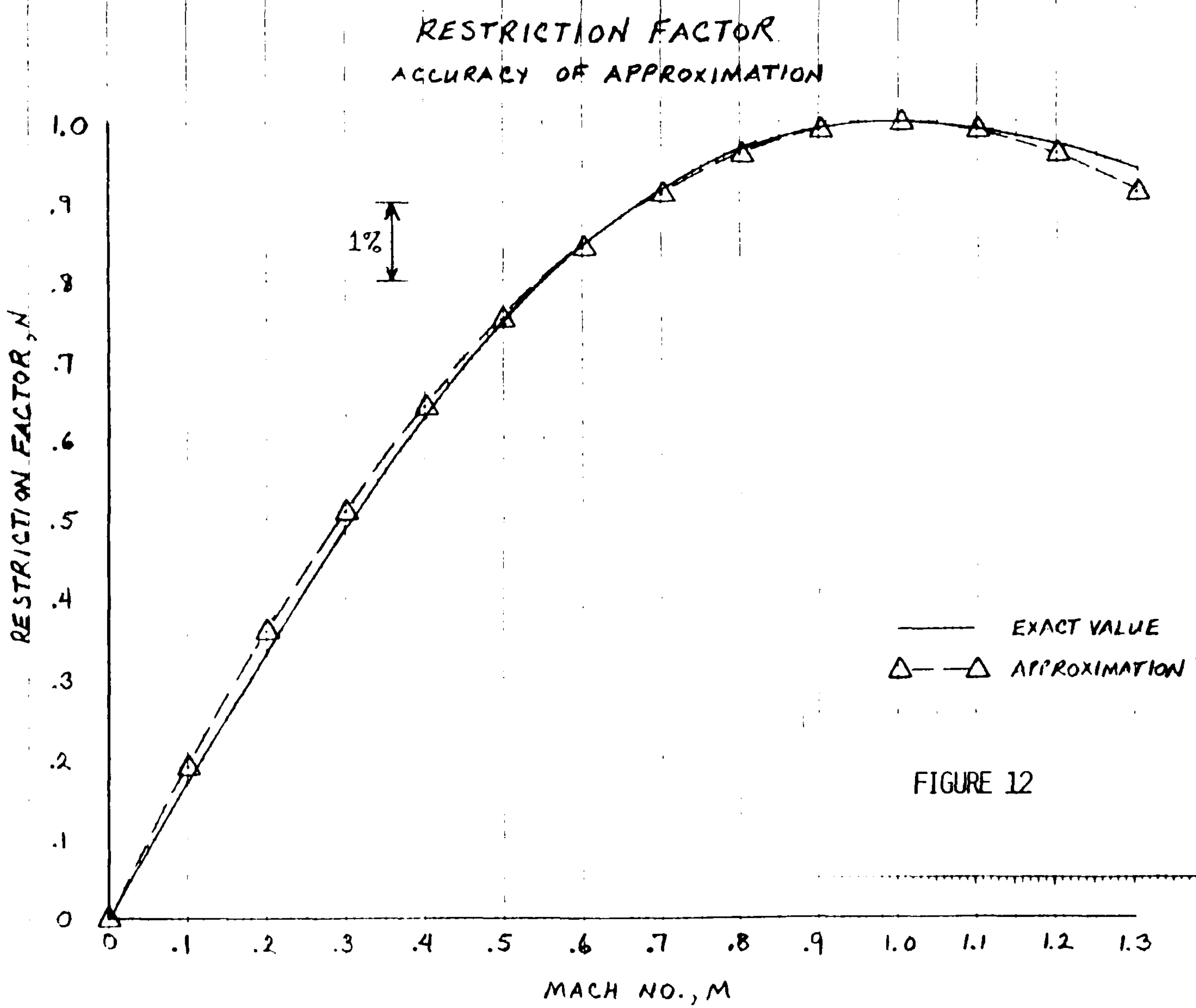
RESTRICTION FACTOR
ACCURACY OF APPROXIMATION
RESTRICTION FACTOR, N
1.0
.9
.8
.7
.6
.5
.4
.3
.2
.1
0
1%
0
.1
.2
.3
.4
.5
.6
.7
.8
.9
1.0
1.1
1.2
1.3
MACH NO., M
EXACT VALUE
APPROXIMATION

FIGURE 12

where $Z_2 = .5M_5(2 - M_5)/(1 - M_5)$.

Since static pressures, ΔP_{s5} and ΔP_{s13} are equal,

$$\Delta P_{13} - \Delta N_{16}Z_1 = \Delta P_5 - \Delta N_5 Z_2. \quad (33)$$

Recalling the relationships in Equations (1), (2), (6) and (7a), Equation (33), can be written as

$$\Delta T_{13}((1+Z_1)GNFD - Z_1/2) - \Delta T_5(Z_2/GNT-.5) + 1/GNT)$$

$$= \Delta W_2 Z_1(1+B)/B + \Delta W_{25}(1-1/B) - \Delta T_4(1/GNT-.5) \quad (34)$$

This is the final form to be used in the second continuity relationship.

Finally, the relationship between T_{13} and T_{25} can be determined experimentally using the engine cycle deck at the desired flight condition. For a given flight condition,

$$T_{13} = T_{25}^{K_f}$$

where power factor, K_f, is the factor relating T_{13} and T_{25} derived from the cycle deck. Taking the log/deriviative,

$$\Delta T_{13} = \Delta T_{25}(K_f). \quad (35)$$

Equations (28), (34), and (35), when combined, give an important transformation matrix of the form,

$$[G][V] = [H][W] + [J][U], \quad (36)$$

where,

$$[V] = \begin{bmatrix} \Delta T_{13} \\ \Delta T_5 \\ \Delta T_{25} \end{bmatrix}, [W] = \begin{bmatrix} \Delta W_2 \\ \Delta W_{25} \\ \Delta T_4 \end{bmatrix}, \text{ and } [U] = \begin{bmatrix} \Delta W_f \\ \Delta A_8 \end{bmatrix}. \quad (37)$$

Rewriting Equation (36) as,

$$[V] = [G]^{-1}[H][W] + [G]^{-1}[J][U] \quad (38a)$$

Equation (38a) will be substituted into Equation (18) in place of the [V] matrix.

The other transformation needed is between the [X] and [W] matrix. This is obtained from the fan and compressor maps. Fan and compressor maps are experimentally derived functions of flow versus pressure ratio along constant rotor speed lines. The cycle deck uses these maps to define an operating point (an air flow and pressure ratio). From these maps, around small equilibrium operating points, air flow can be considered a linear function of pressure ratio and speed. For the fan and compressor this means,

$$\Delta W_2 = \Delta N_1 (DW2QN) + \Delta P_{13}(DWQP)$$
$$\Delta W_{25} = \Delta N_{25} (DWCQN) + \Delta P_3 QP_{25}(DWCQP),$$

where DW2QN, DWQP, DWCQN, and DWCQP and linear derivatives derived from the cycle deck. From Equation (2), (5b), (6), and the definition that

$$\Delta P_3 QP_{25} = \Delta P_3 - \Delta P_{25},$$

the equations can be rewritten as,

$$\Delta W_2 = \Delta N_1 (DW2QN) + \Delta T_{13}(DWQP)(GNFD)$$
$$\Delta W_{25} = \frac{1}{DWCQP} \left[\Delta N_2 (DWCQN) + \Delta T_4 (DWCQP) - \Delta T_{25}(DWCQP)(GNF)\right]$$

In matrix form, the above equations are,

$$\begin{bmatrix} \Delta W_2 \\ \Delta W_{25} \\ \Delta T_4 \end{bmatrix} = [DWX] \begin{bmatrix} \Delta N_1 \\ \Delta N_2 \\ \Delta T_4 / K_4 \end{bmatrix} + [DWV] \begin{bmatrix} \Delta T_{13} \\ \Delta T_5 \\ \Delta T_{25} \end{bmatrix} \qquad (38b)$$

which are of the form,

$$[W] = [DWX][X] + [DWV][V],$$

where,

$$DWX = \begin{bmatrix} DW2QN & 0 & 0 \\ 0 & \dfrac{DWCQN}{(1-DWCQP)} & \dfrac{K_4(DWCQP)}{2(1-DWCQP)} \\ 0 & 0 & K_4 \end{bmatrix} \quad \text{and}$$

$$DWV = \begin{bmatrix} DWQP(GNFD) & 0 & 0 \\ 0 & 0 & \dfrac{1}{(1-DWCQP)}[-DWCQP(GNF)] \\ 0 & 0 & 0 \end{bmatrix}$$

The transformation matrices of Equations (38a) and (38b) can now be substituted into Equation (18) to obtain the conventional form of,

$$[\dot{X}] = [A][X] + [B][U].$$

The final form of Equation (18) after the transformation substitutions is,

$$\begin{aligned} [\dot{X}] = {} & (A + EG^{-1}H)[I - [DWV][G^{-1}H]][DWX][X] + \\ & [(A + EG^{-1}H)[I - [DWV](G^{-1}H)]^{-1}[DWV](G^{-1}J) + \\ & (B + EG^{-1}J)][U] \end{aligned} \quad (39)$$

where [I] is the identity matrix.

Equation (39) is in the proper state space format.

Error Analysis

The error analysis will include consideration of the assumptions in the development of the analytic state space model and errors induced into the model with the use of the transformation matrices.

One important assumption used in the development of the analytic equations was that ΔP_3 is equal to ΔP_4. This assumption is based on

the ratio P_3/P_4 being nearly constant over the range of turbofan engine operation of concern. When the log/derivative is taken the assumed result is achieved. The other important assumption made was that ΔT_4 the HPT inlet temperature, is equal to ΔT_{42}, LPT inlet temperature. This assumption is based on the nearly constant HPT efficiency over a wide range of engine operating conditions. The assumption was tested using engine cycle deck data. Over the range of 35 degrees PLA to 70 degrees PLA, the ratio of ΔT_4 to ΔT_{42} was .983 ± .015 verifing the accuracy of the assumption.

The assumptions made in deriving Equations (25a) and (25b) were based on past engine experience and common practice when combining two separate air flows like W_{13} and W_{25}. The accuracy of mass weighting temperatures when combining air flows is seen in Figure 13a which plots T_8 calculated using the cycle deck versus T_8 approximated by mass weighting. The slope of the line is nearly one giving strength to the approximation. However, when the log/derivative is taken, the accuracy of the resulting Equation (25a) is reduced to approximately 80% over the range of engine operation. Equation (25b), however, proves much more accurate in its approximation of pressure addition of two flows. Figure 13b shows a plot of ΔP_8 as calculated by the cycle deck versus ΔP_8 as calculated by Equation 25b. Again, the slope is nearly one, confirming the accuracy of the approximation.

The largest error in computing the elements of the analytic state space model come from the numerous substitutions and transformation matrices used to reduce the analytic model to a 3 by 3 state space. The errors are large enough to require the user to rely on the empirically derived state space models for accurate modeling of engine transient

FIGURE 13A

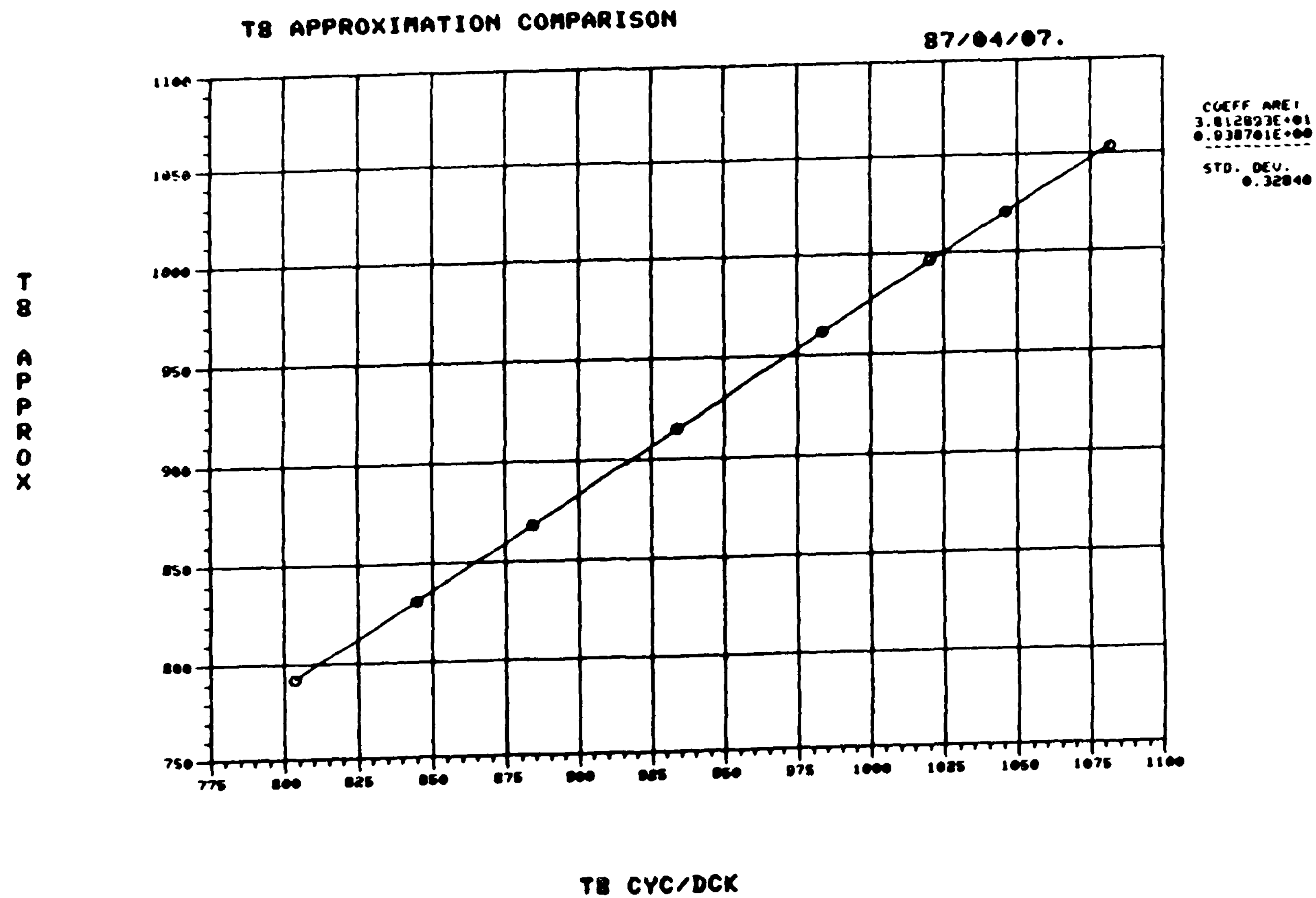

T8 APPROXIMATION COMPARISON
87/04/07.
COEFF ARE:
3.812893E+01
0.938701E+00
STD. DEV.
0.32840
T8 APPROX
T8 CYC/DCK
1100
1050
1000
950
900
850
800
750
775
800
825
850
875
900
925
950
975
1000
1025
1050
1075
1100

FIGURE 13B

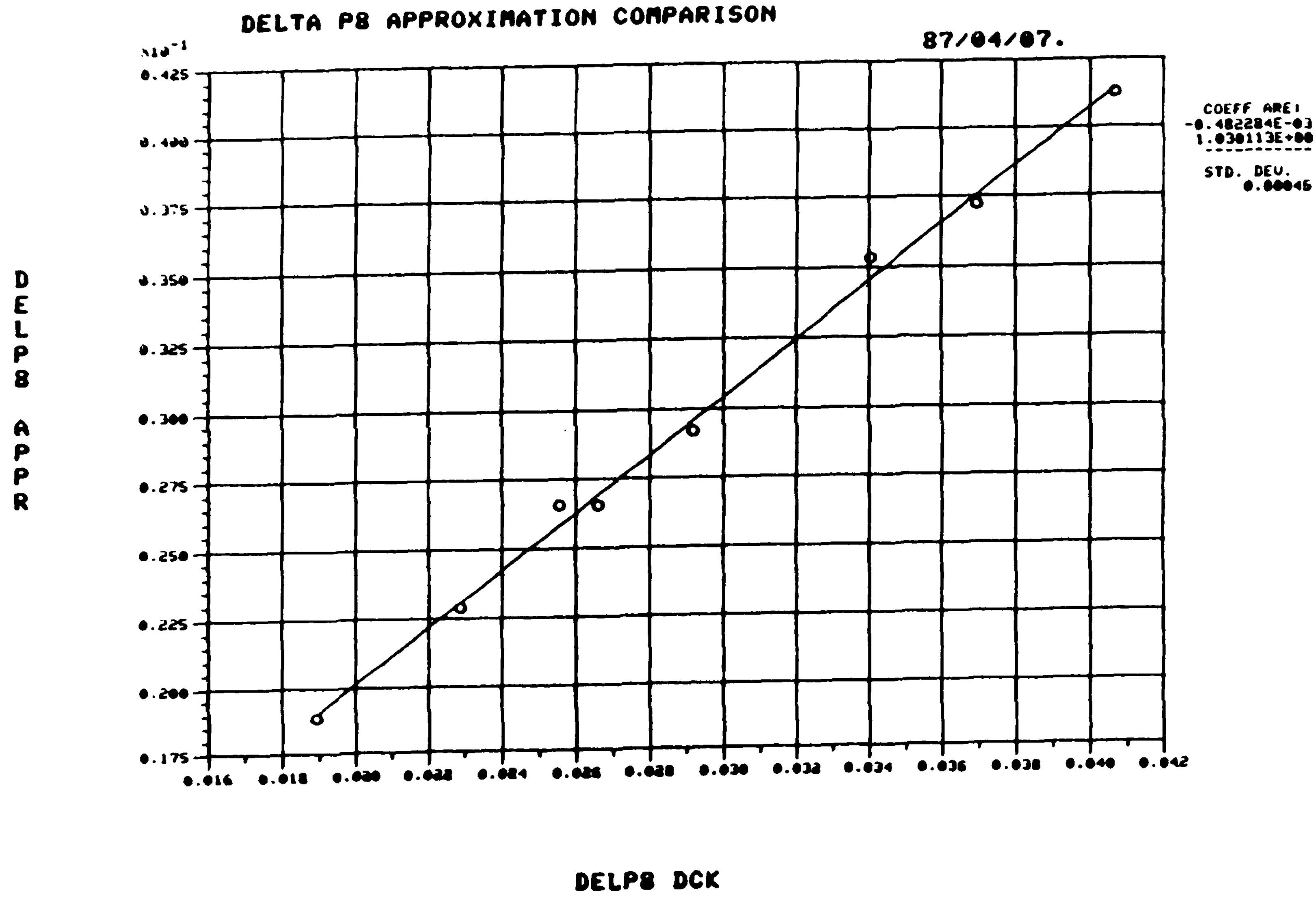
DELTA P8 APPROXIMATION COMPARISON
87/04/07.
x10^-1
0.425
0.400
0.375
0.350
0.325
0.300
0.275
0.250
0.225
0.200
0.175
0.016
0.018
0.020
0.022
0.024
0.026
0.028
0.030
0.032
0.034
0.036
0.038
0.040
0.042
COEFF ARE:
-0.482284E-03
1.030113E+00
STD. DEV.
0.00045
DELP8 APPR
DELP8 DCK

characteristics and the analytic models for insight into individual engine parameter effects on transient performance

Comparison of the analytic versus the empirical state space models show the substantial differences. Keep in mind, however, the form of the empirical equations and the form of the analytic equations. The states of the analytic equations were defined as

$$\Delta X = \frac{dX}{X_e} .$$

For comparison, it is necessary to multiply row 1 of the [B] matrix of Equation (39) by N_{1e}, row 2 by N_{2e} and row 3 by T_{4e}. Then, multiplying columns 1 and 2 of the [B] matrix by W_{fe} and A_{8e} respectively, will put the analytic form of the equations into the empirical form.

V Engine Control Design

Using the analytic equations described above, state space equations were derived at various PLA settings starting with 35 degrees to 70 degrees in 5 degree increments. Table I compares the analytic state space models with the previously derived empirical state space models for each PLA setting. The errors induced by numerous substitutions and transformation matrices do not give good correlation between to two.

There is one important insight the analytic state space models do give. The [B] matrix of the analytic equations shows that $\dot{T}_4$ is the only parameter affected directly by fuel flow inputs. The empirical state space models, however, show small effects of fuel flow inputs on $\dot{N}_1$ and $\dot{N}_2$. Upon closer examination of the root locus plots generated from the empirical equations, (see Figures 3 through 10), a large negative zero is generated. If, in the empirical equations, the elements B(1,1) and B(1,2) of the [B] matrix are set equal to zero corresponding to analytic values, the large zero characteristic in each of the the root locus plots disappears. The loss of the large zero does not affect the characteristcs of the empirical state space models. However, due to the differences in the empirical and analytic values, it is necessary to use the empirical form in developing feedback control logic. The analytic equations can still be used to understand trends and the effects of specific parameters on engine performance.

The reason for the large negative zero is understood when examining the accuracy of convergence routines used today in non-linear engine cycle decks to balance energy and continuity as discussed previously. The convergence subroutine works by equating changes in N_1, N_2, T_4, W_f, and A_8 with off-torques, $\dot{N}_1$ and $\dot{N}_2$, and $\dot{T}_4$. The convergence subroutine

TABLE I

EMPERICAL / **ANALYTICAL**

PLA=70

EMPERICAL:

$$A = \begin{matrix} -8.856 & 3.333 & 4.179 \\ 1.240 & -3.031 & 5.425 \\ -.0385 & -.129 & -1.099 \end{matrix} \qquad B = \begin{matrix} .0472 & 21.362 \\ .0380 & -2.394 \\ .148 & .654 \end{matrix}$$

ANALYTICAL:

$$A = \begin{matrix} -2.056 & .728 & .502 \\ .207 & -.241 & .584 \\ .0377 & -.388 & -1.547 \end{matrix} \qquad B = \begin{matrix} 0 & 30.782 \\ 0 & -7.286 \\ .403 & -.282 \end{matrix}$$

PLA=65

EMPERICAL:

$$A = \begin{matrix} -8.582 & 3.527 & 3.978 \\ 1.153 & -3.159 & 5.112 \\ -.105 & -.139 & -1.050 \end{matrix} \qquad B = \begin{matrix} .0456 & 20.500 \\ .0374 & -2.471 \\ .153 & .488 \end{matrix}$$

ANALYTICAL:

$$A = \begin{matrix} -1.676 & .770 \\ .172 & -.250 \\ .0313 & -.339 \end{matrix} \qquad B = \begin{matrix} 0 & 34.251 \\ 0 & -8.051 \\ .429 & -.308 \end{matrix}$$

PLA=60

EMPERICAL:

$$A = \begin{matrix} -10.662 & 7.130 & 3.729 \\ 1.292 & -4.332 & 4.893 \\ -.0206 & -.362 & -1.013 \end{matrix} \qquad B = \begin{matrix} .0426 & 20.751 \\ .0354 & -1.983 \\ .157 & .331 \end{matrix}$$

ANALYTICAL:

$$A = \begin{matrix} -1.563 & .455 & .447 \\ .157 & -.147 & .586 \\ .0230 & -.196 & -1.531 \end{matrix} \qquad B = \begin{matrix} 0 & 34.876 \\ 0 & -7.988 \\ .453 & -.243 \end{matrix}$$

PLA=55

EMPERICAL:

$$A = \begin{matrix} -8.515 & 4.594 & 3.423 \\ .692 & -2.207 & 4.532 \\ -.00218 & -.256 & -.941 \end{matrix} \qquad B = \begin{matrix} .0425 & 19.045 \\ .0319 & -1.050 \\ .163 & .320 \end{matrix}$$

ANALYTICAL:

$$A = \begin{matrix} -1.972 & .454 & .422 \\ .197 & -.146 & .585 \\ .269 & -.189 & -1.523 \end{matrix} \qquad B = \begin{matrix} 0 & 37.11 \\ 0 & -8.363 \\ .483 & -.233 \end{matrix}$$

PLA=50

EMPERICAL:

$$A = \begin{matrix} -7.487 & 4.258 & 3.264 \\ .578 & -1.951 & 3.983 \\ -.0188 & -.237 & -.865 \end{matrix} \qquad B = \begin{matrix} .0449 & 14.966 \\ .0296 & -.500 \\ .172 & -.307 \end{matrix}$$

ANALYTICAL:

$$A = \begin{matrix} -2.104 & .442 & .383 \\ .201 & -.140 & .581 \\ .0259 & -.173 & -1.510 \end{matrix} \qquad B = \begin{matrix} 0 & 40.725 \\ 0 & -8.804 \\ .563 & -.226 \end{matrix}$$

PLA=45

EMPERICAL:

$$A = \begin{matrix} -3.500 & 1.735 & 2.959 \\ -.147 & -.620 & 3.318 \\ -.0506 & -.100 & -.762 \end{matrix} \qquad B = \begin{matrix} .0478 & 11.017 \\ .0248 & .623 \\ .183 & .339 \end{matrix}$$

ANALYTICAL:

$$A = \begin{matrix} -3.686 & .0795 & .210 \\ .328 & -.0233 & .585 \\ .0404 & -.0269 & -1.493 \end{matrix} \qquad B = \begin{matrix} 0 & 53.044 \\ 0 & -10.676 \\ .660 & -.254 \end{matrix}$$

TABLE I - CONT'D NEXT PAGE

TABLE I-CONT'D

EMPERICAL | **ANALYTICAL**

PLA=40

$$A = \begin{bmatrix} -3.995 & 3.281 & 2.640 \\ -.1738 & -1.219 & 3.049 \\ -.0101 & -.185 & -.695 \end{bmatrix} \quad B = \begin{bmatrix} .0454 & 10.484 \\ .0258 & -.00534 \\ .194 & .222 \end{bmatrix} \qquad A = \begin{bmatrix} -4.505 & .541 & .0465 \\ .381 & -.150 & .587 \\ .0508 & -.161 & -1.478 \end{bmatrix} \quad B = \begin{bmatrix} 0 & 64.120 \\ 0 & -12.454 \\ .750 & -.314 \end{bmatrix}$$

PLA=35

$$A = \begin{bmatrix} -2.570 & 1.226 & 2.265 \\ -.130 & -.416 & 2.741 \\ -.0212 & -.068 & -.618 \end{bmatrix} \quad B = \begin{bmatrix} .0442 & 7.445 \\ .0268 & .732 \\ .206 & .241 \end{bmatrix} \qquad A = \begin{bmatrix} -6.872 & 1.268 & -.330 \\ .554 & -.313 & .500 \\ .0893 & -.303 & -1.456 \end{bmatrix} \quad B = \begin{bmatrix} 0 & 88.255 \\ 0 & 16.698 \\ .871 & .495 \end{bmatrix}$$

does not know that N_1 and N_2 are not directly affected by W_f and, by its nature must generate small off-torque values $\dot{N}_1$, and $\dot{N}_2$, for a given change in W_f. Although the error is small it manifests itself in a large negative, non-effective root.

Using the empirically derived state space matrices between 35 degrees PLA and 70 degrees PLA, feedback control systems were derived to improve the F101 engine response to small changes in PLA.

The present control logic internal to the engine cycle deck simulation involves the feedback of the fuel metering valve rate, and N_2. For PLA changes of 2 degrees, response is on the order of 3 seconds to reach steady state values.

The present feedback control logic installed in the engine cycle deck had to be bypassed and a new feedback logic using a lead/lag filter equivalent to a N_2 and $\dot{N}_2$ feedback was installed. The lead/lag filter was used to control to a desired gain margin for tracking error and to increae phase margin for increased engine response time. With a new control feedback system based on the empirical state space models, response was improved up to 75% in rise time. Figure 14 illustrates the new feedback system. N_2 was used specifically for the F101 because the F101 is controlled by a N_2 control schedule which is specified by a PLA setting. In an engine like the F110, which is controlled by an N_1 schedule based on a PLA setting, N_1 and $\dot{N}_1$ could have been fed back.

Table II tabulates the gains on the rate, $\dot{N}_2$, and N_2 feedback for various PLA settings. Also listed in Table II is the percent increase in response times to 90% steady state values. Figures 15a through 15h show the increases in the response of N_2 over the present transient cycle deck model.

FIGURE 14 SCHEMATIC OF NEW FEEDBACK CONTROL SYSTEM. SEE TABLE II FOR A, B, K_B VALUES.

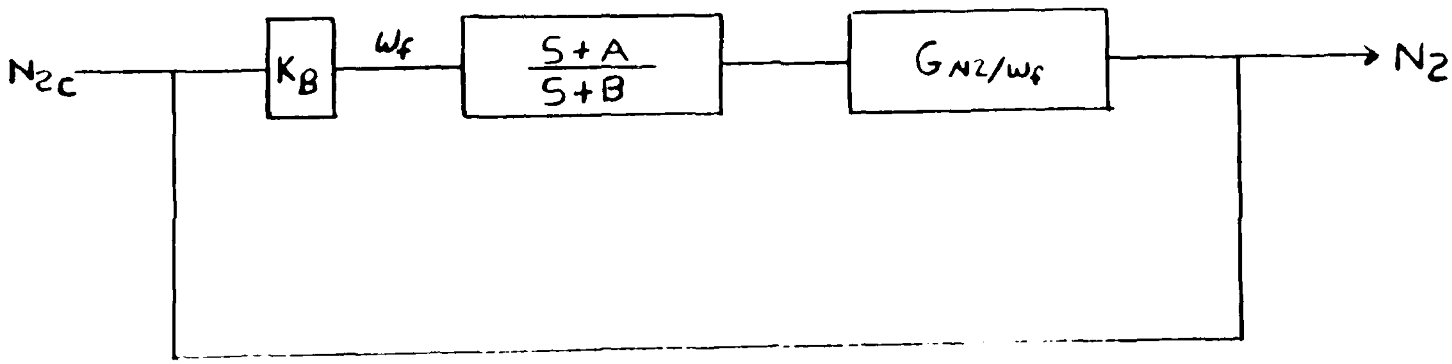

PLA	A	B	K_B	% INCREASE RISE TIME
70	3	10	30.0	39.0
65	3	10	25.0	34.0
60	3	10	20.0	25.0
55	3	10	20.0	24.0
50	3	10	20.0	24.3
45	3	10	12.5	16.0
40	3	10	10.0	7.0
35	3	10	5.0	13.0

TABLE II GAINS AND % INCREASE IN RISE TIME OF N_2, $\dot{N}_2$ FEEDBACK **VERSUS** PRESENT CYCLE DECK

Figure 15A N2 (Core Speed) .vs. Time, PLA = 35 Degrees

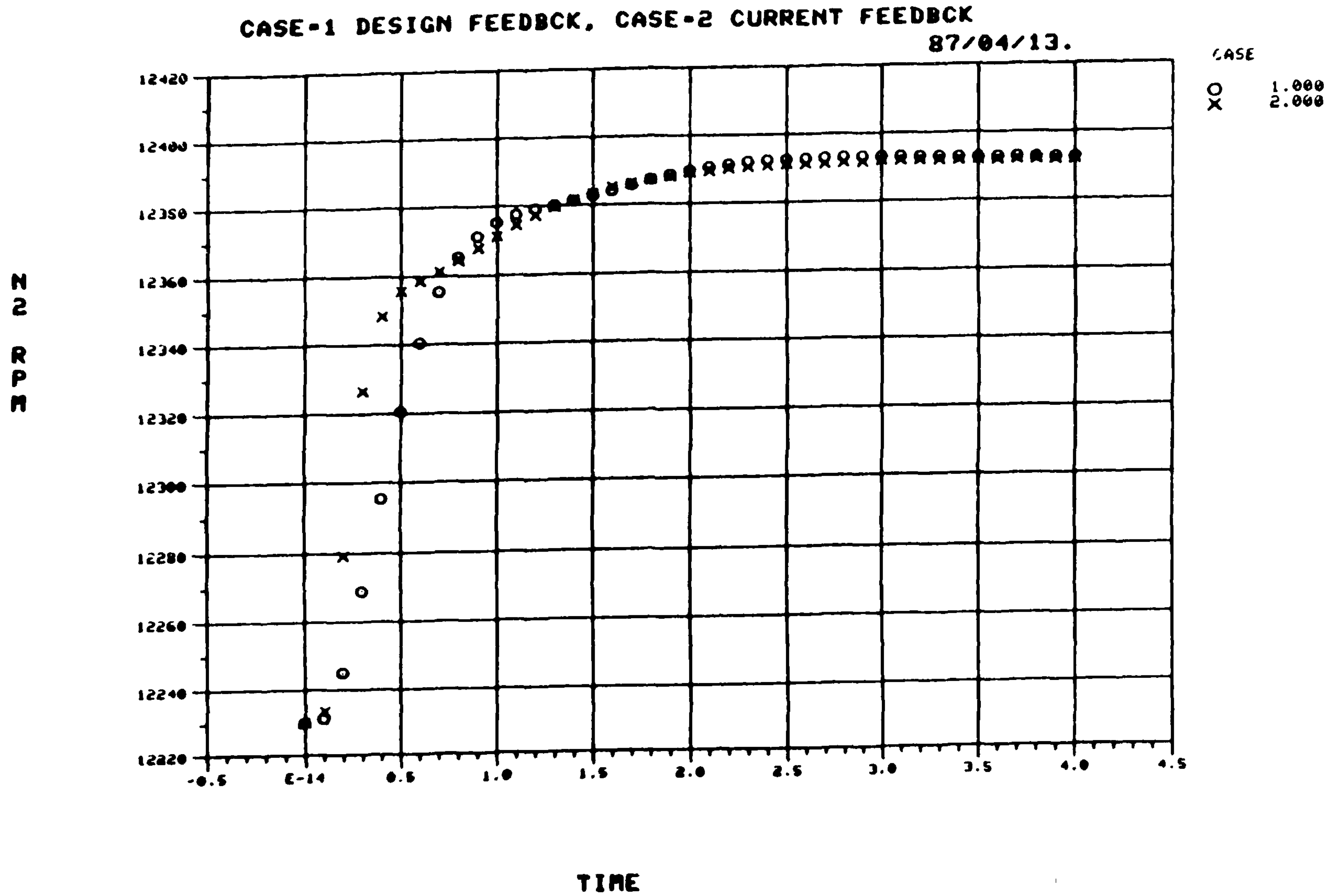

FIGURE 15B N2 (CORE SPEED) .VS. TIME, PLA = 40 DEGREES

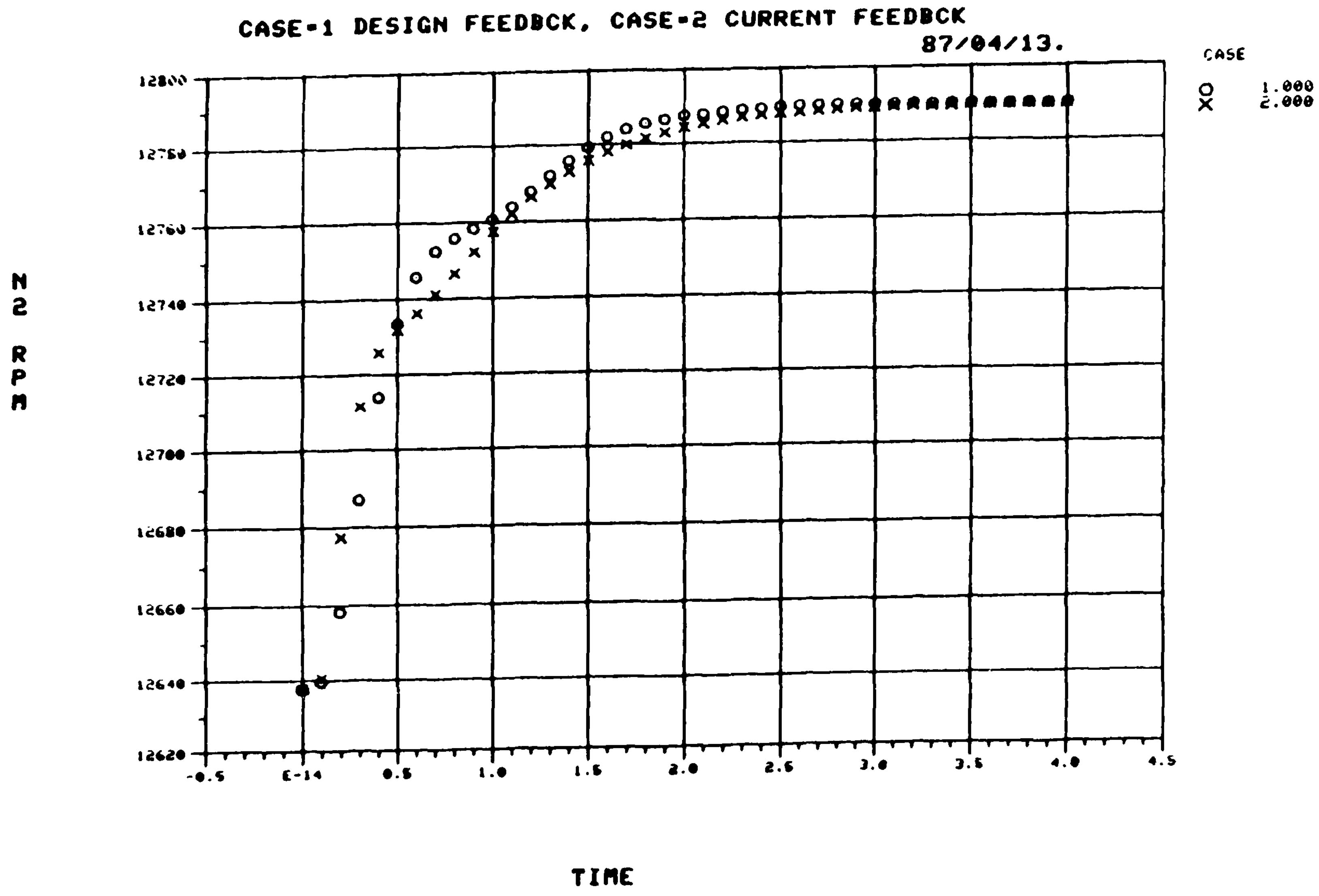

FIGURE 15c N2 (CORE SPEED) .VS. TIME, PLA = 45 DEGREES

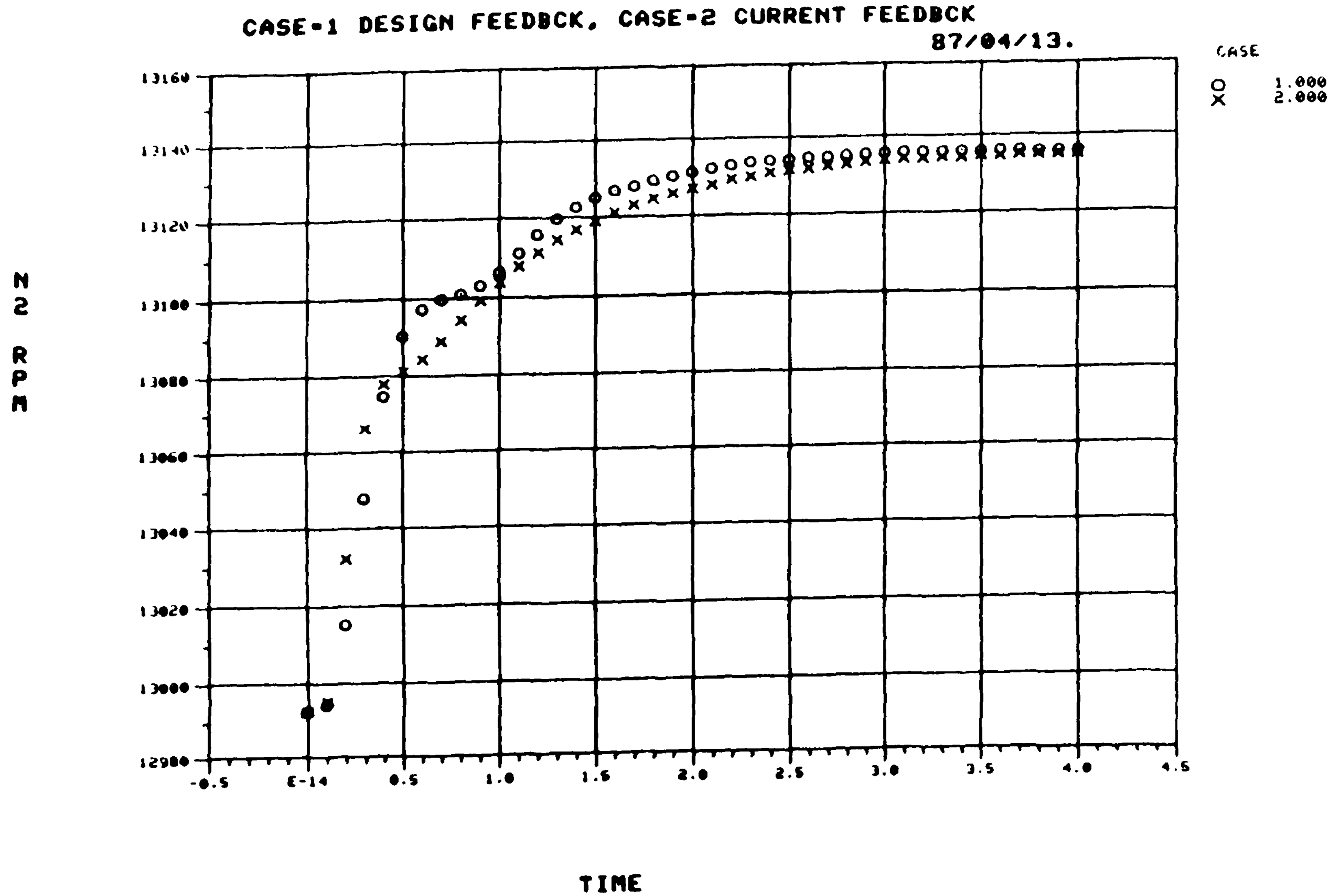

FIGURE 15D N2 (CORE SPEED) .VS. TIME, PLA = 50 DEGREES

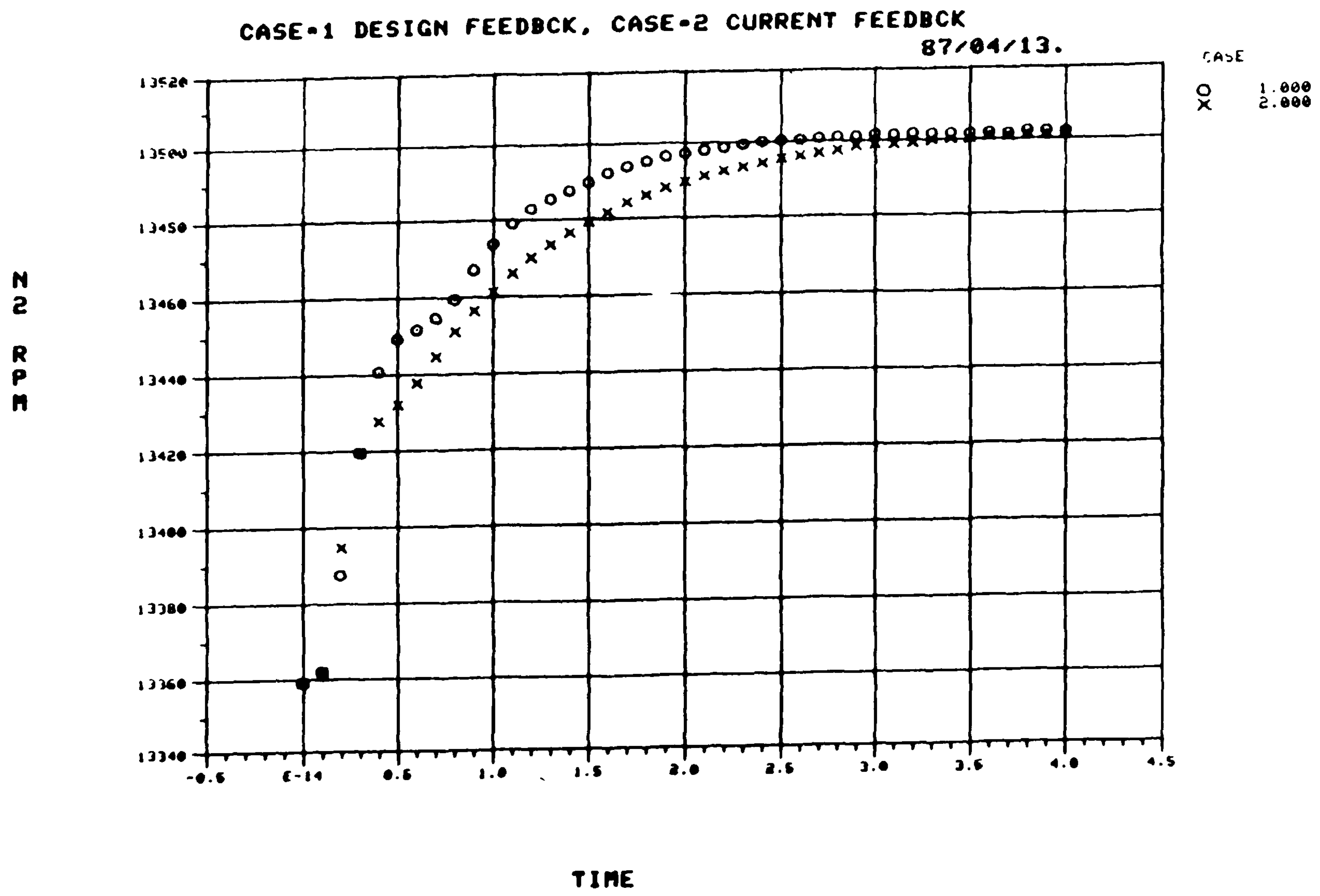

FIGURE 15E N2 (CORE SPEED) .VS. TIME, PLA = 55 DEGREES

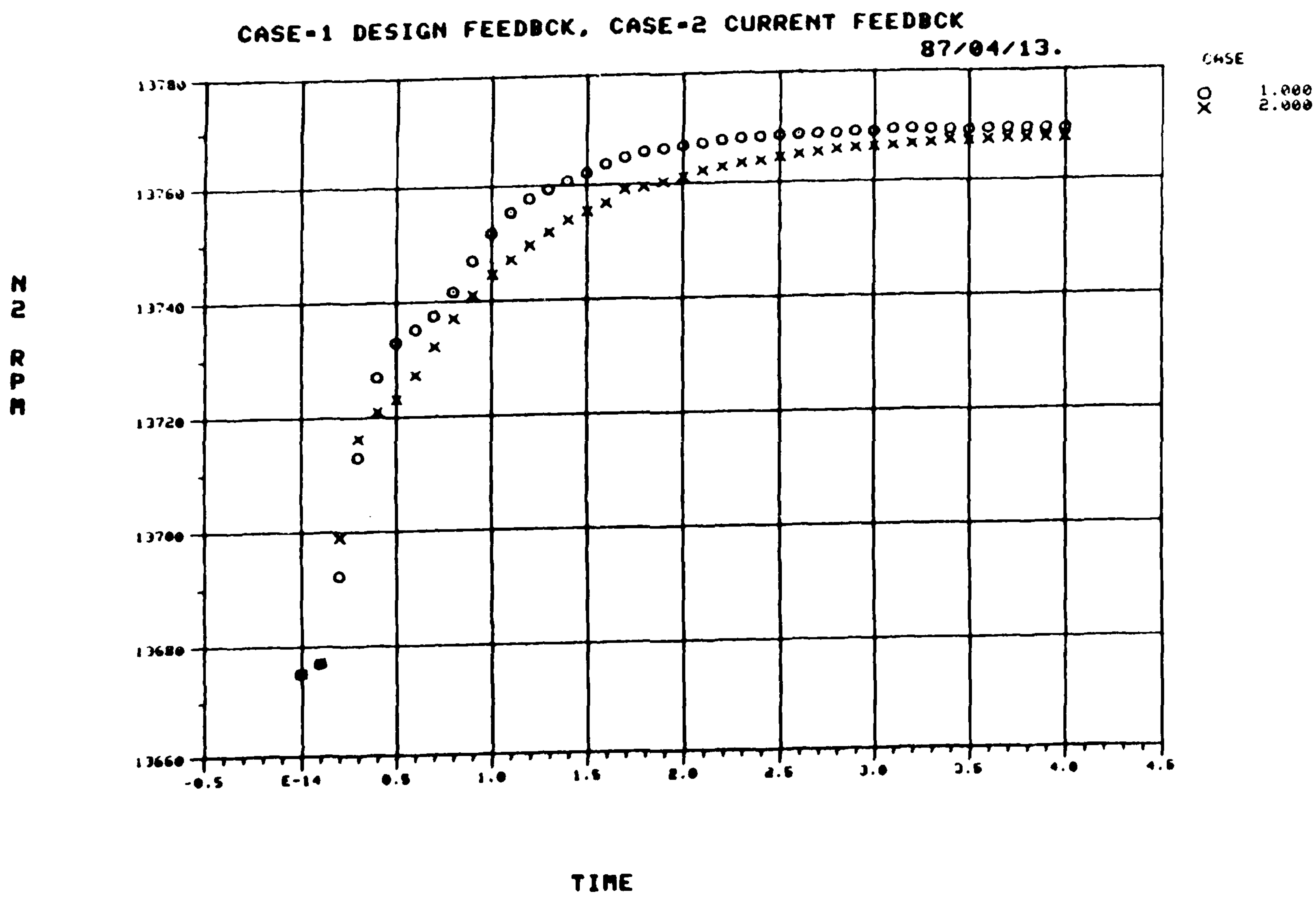

FIGURE 15F N2 (CORE SPEED) .VS. TIME, PLA = 60 DEGREES

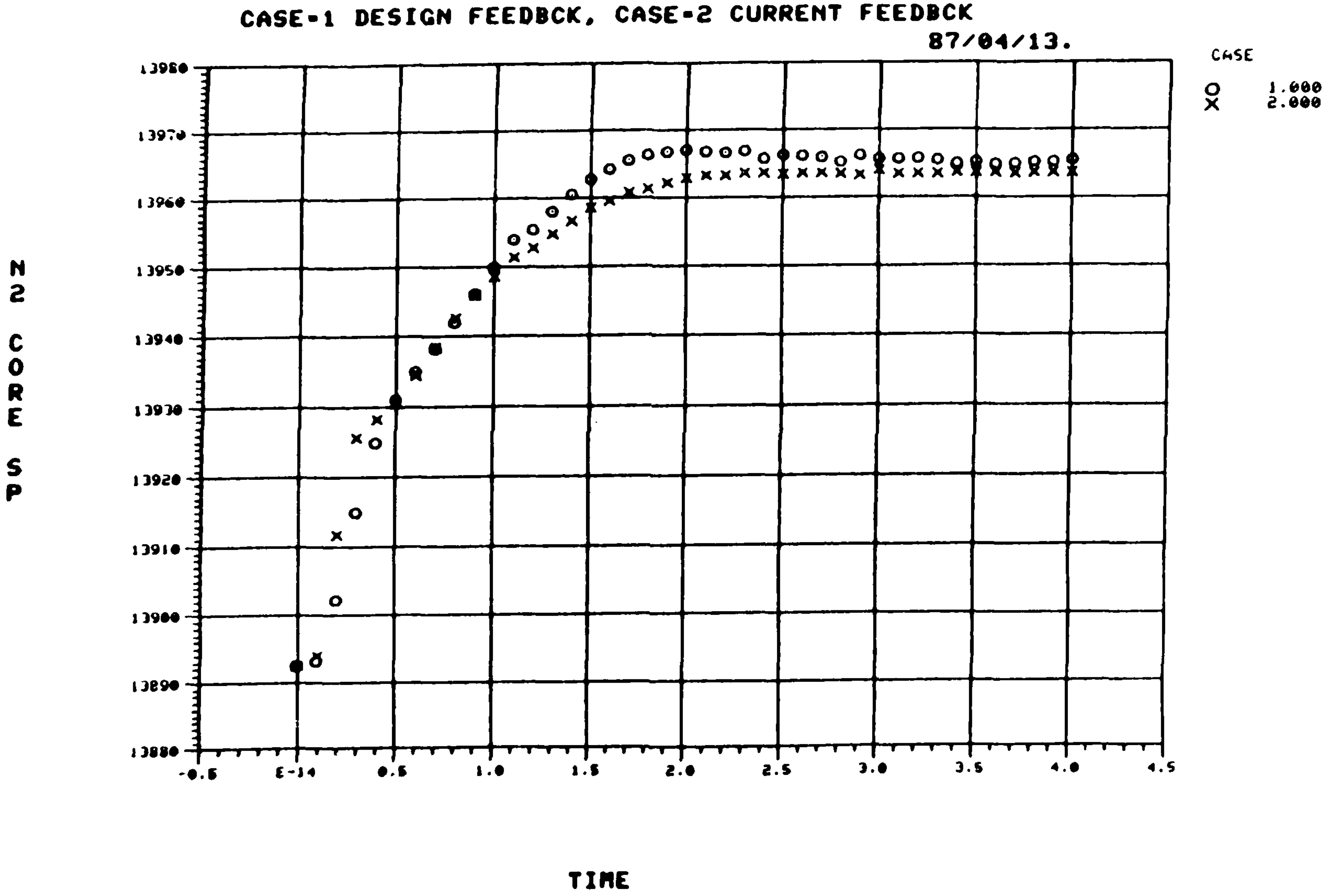

FIGURE 15G N2 (CORE SPEED) .VS. TIME, PLA = 65 DEGREES

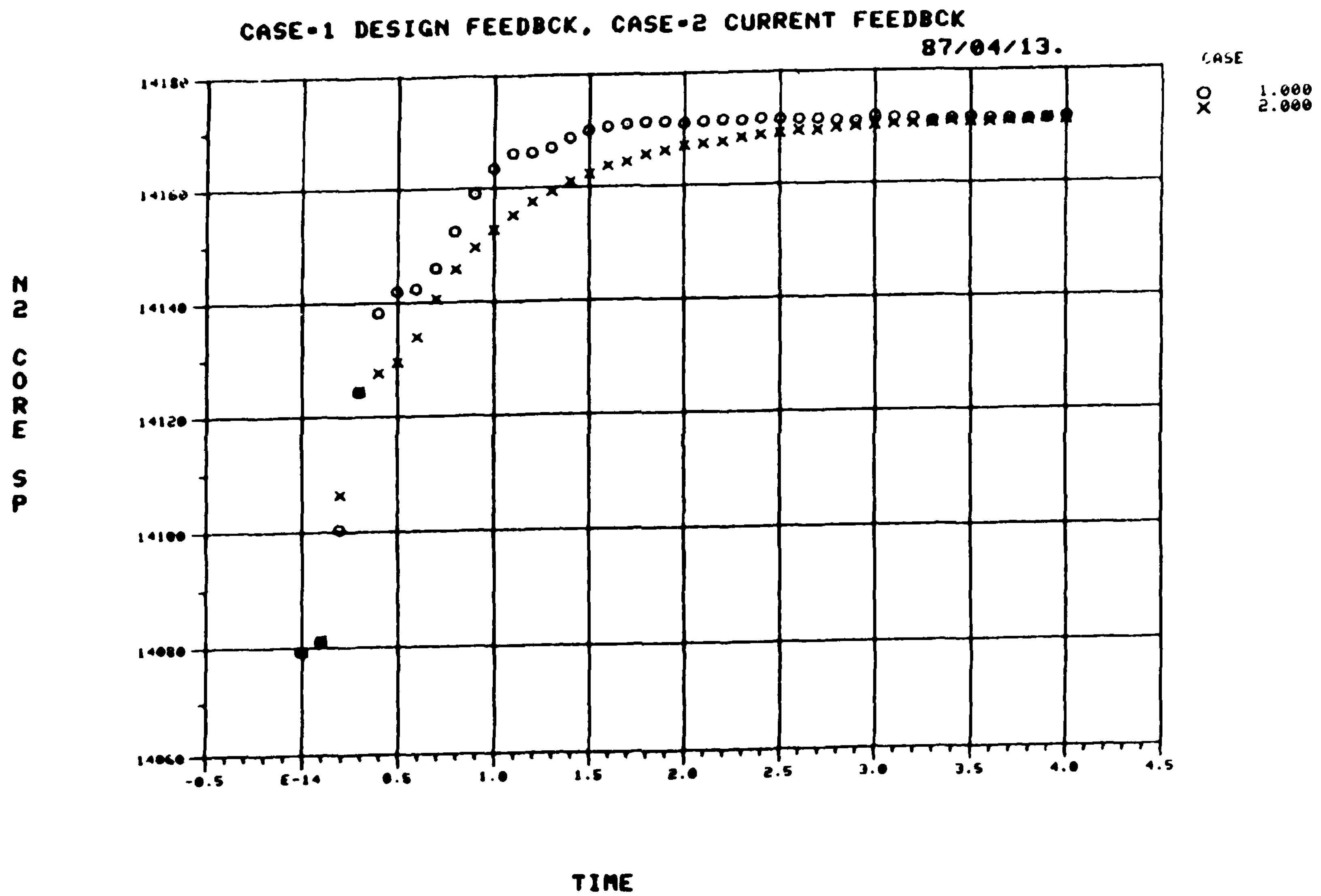

FIGURE 15H N2 (CORE SPEED) .VS. TIME, PLA = 70 DEGREES

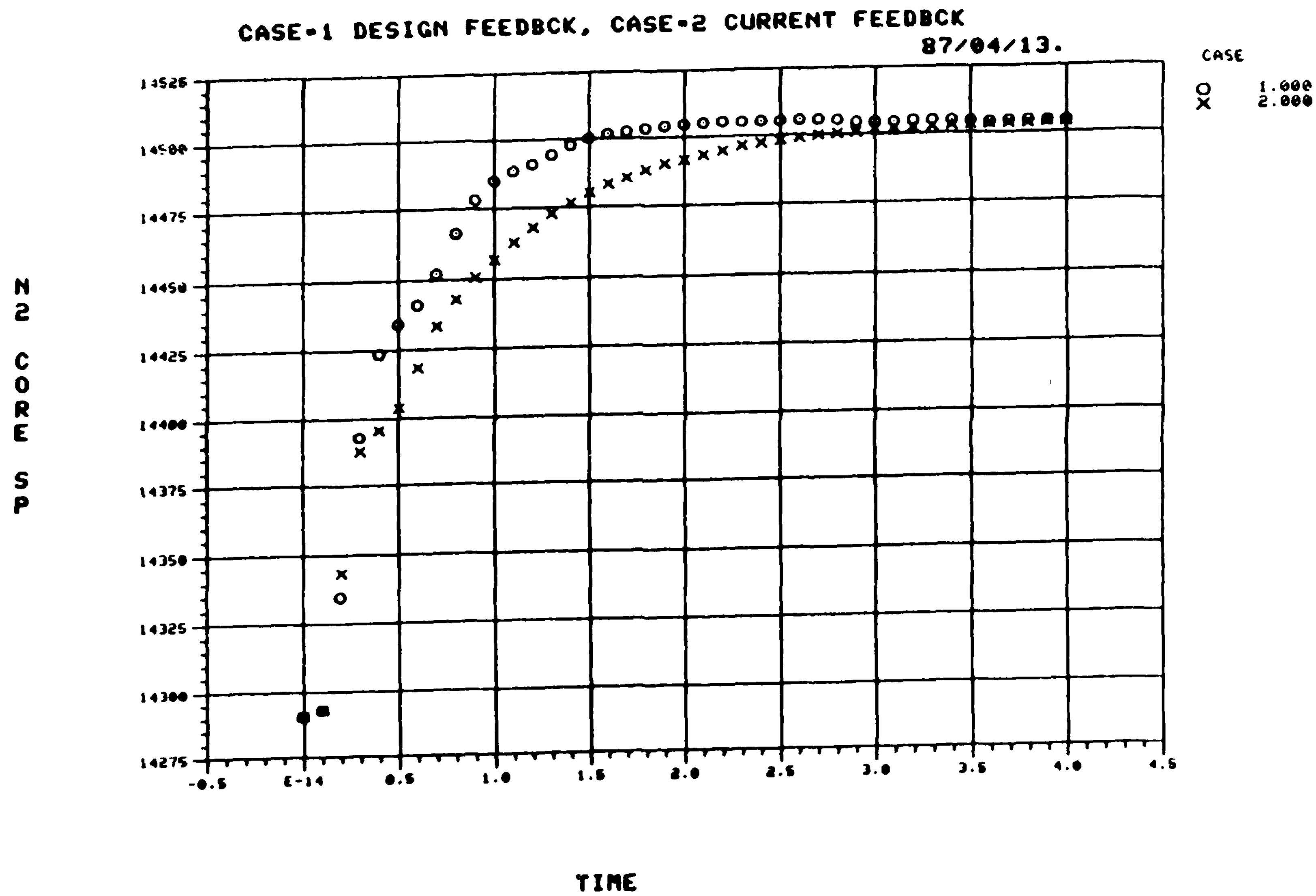

IV Conclusions

The analytic equations offer a means of visualizing the effects of individual parameters on engine performance but are too numerically inaccurate to be used in modeling transient engine performance. Emperical equations, however, offer accurate state space models for the developement of engine feedback control logic.

Using the empirical state space models to develop new feedback control logic, the F101 transient performance was improved over present engine performance for small changes in PLA.

Bibliography

1. Wills TK. Operating Instructions for the F101 - GE - 102 Steady State Performance Computer Program. General Electric Corporation, 1986.

2. ASD/ENFPA. "Control Systems Analysis," Class Notes and Problems used for branch training, 1968-1969.

3. H. Brown. Analytic Partials Model. Advanced Engineering Technology Department Technical Memorandum. General Electric Corporation, Sept., 1986.

VITA

Greg Thelen was born in Melrose, Minnesota, on 26 October, 1958. He graduated from Melrose Sr. High School in 1977 and attended the University of Minnesota from which he received a B.S. in Aerospace Engineering in March 1982. He entered the USAF in October 1982 and has been stationed at Wright Patterson AFB, Ohio, since August 1983. He is currently working for ASD/ENFPA as lead propulsion performance engineer.

SECURITY CLASSIFICATION OF THIS PAGE

REPORT DOCUMENTATION PAGE

Form Approved
OMB No. 0704-0188

1a. REPORT SECURITY CLASSIFICATION UNCLASS	1b. RESTRICTIVE MARKINGS
2a. SECURITY CLASSIFICATION AUTHORITY	3. DISTRIBUTION / AVAILABILITY OF REPORT Approved for public release; distribution unlimited.
2b. DECLASSIFICATION / DOWNGRADING SCHEDULE	
4. PERFORMING ORGANIZATION REPORT NUMBER(S)	5. MONITORING ORGANIZATION REPORT NUMBER(S)
6a. NAME OF PERFORMING ORGANIZATION ASD/ENFPA	6b. OFFICE SYMBOL *(If applicable)* ASD/ENFPA
7a. NAME OF MONITORING ORGANIZATION	
6c. ADDRESS *(City, State, and ZIP Code)* WPAFB, OH 45433	7b. ADDRESS *(City, State, and ZIP Code)*
8a. NAME OF FUNDING / SPONSORING ORGANIZATION	8b. OFFICE SYMBOL *(If applicable)*
9. PROCUREMENT INSTRUMENT IDENTIFICATION NUMBER	
8c. ADDRESS *(City, State, and ZIP Code)*	10. SOURCE OF FUNDING NUMBERS

PROGRAM ELEMENT NO.	PROJECT NO.	TASK NO	WORK UNIT ACCESSION NO.

11. TITLE *(Include Security Classification)*

12. PERSONAL AUTHOR(S)
Capt Gregory L. Thelen

13a. TYPE OF REPORT	13b. TIME COVERED	14. DATE OF REPORT *(Year, Month, Day)*	15. PAGE COUNT
Final	FROM May 86 TO Dec 87	87/12/1	

16. SUPPLEMENTARY NOTATION

17. COSATI CODES		
FIELD	GROUP	SUB-GROUP

18. SUBJECT TERMS *(Continue on reverse if necessary and identify by block number)*

Linearization of a Turbofan Engine

Approved for public release: IAW AFR 190
24 Feb 88

19. ABSTRACT *(Continue on reverse if necessary and identify by block number)*

Present generation trubofan engines use hydro/mechanical control governors to regulate fuel flow and control engine performance. State-of-the-Art and future engines will have the ability to use digital control logic to control engine performance. Due to these advances in engine control capability, there is a need to linearly model the turbofan engines and develop control systems to understand and optimize engine performance. This paper will describe the means of developing linear state space models which model transient turbofan engine performance.

The F101 turbofan engine, used on the B-1B bomber, will be used as an example with the linear state space models being derived from the non-linear F101 engine computer simulation model. The internal convergence logic of the F101 engine simulation will be used to derive the individual elements making up the linear state space models. The

20. DISTRIBUTION / AVAILABILITY OF ABSTRACT ☒ UNCLASSIFIED/UNLIMITED ☐ SAME AS RPT ☐ DTIC USERS	21. ABSTRACT SECURITY CLASSIFICATION Unclass
22a. NAME OF RESPONSIBLE INDIVIDUAL [illegible] Thelen	22b. TELEPHONE *(Include Area Code)* (513) 255 9472
22c. OFFICE SYMBOL ASD/ENFPA	

DD Form 1473, JUN 86 Previous editions are obsolete. SECURITY CLASSIFICATION OF THIS PAGE

linear state space models will consist of both high speed and low speed rotor dynamics and turbine inlet temperature hear soak dynamics. State space inputs consedered will be fuel flow and engine exit nozzle area. Also discussed in this paper will be linear analytic equations in state space format and their comparative accuracies to the models derived using the F101 non-linear computer simulation model.

Based on the linear state space models developed in this paper, control systems will be designed and implemented into the F101 engine computer model. Transient performance will be compared between current engine control design and the control design based on the linear state space models. Final results will confirm the validity of the state space models derived by showing improvement over current engine transient performance.

END
DATE
FILMED
4-88
DTIC